Int J Mech Mater Des (2024) 20:81–105
https://doi.org/10.1007/s10999-023-09662-9

Dynamic analysis of rectangular cut-out plates resting on elastic foundation

Sabyasachi Ghosh · Subham Pal · Salil Haldar

Received: 22 February 2023 / Accepted: 27 May 2023 / Published online: 20 June 2023

Abstract A finite element method using a 9-node isoparametric plate bending element, incorporating the effects of transverse shear based on the first-order shear deformation theory, is proposed for the free vibration analysis of rectangular cut-out plates resting on an elastic foundation. The elastic foundation is modeled on the Winkler and the Pasternak type, and equations of motion are obtained using the principle of virtual work. To account for the parabolic strain variation through the thickness, a shear correction factor of 5/6 is used, and the effect of rotary inertia has been included in the formulation. The present formulation is compared with established results obtained using analytical methods, with and without rotary inertia, and the max variation observed is 2.24% without rotary inertia and 0.02% with rotary inertia. Cut-out plates are validated with results obtained using the finite element method, and the max variation observed between established results and present formulation is 1.3%. Establishing the accuracy of the current formulation, new results are obtained for rectangular cut-out plates resting on an elastic foundation of various stiffness parameters. The effect of incrementing cut-out dimensions and different layouts of cut-outs in the plate on the free vibration response of plates resting on an elastic foundation is investigated, along with the effects of varying aspect ratios and thickness-to-side ratios.

Keywords Isotropic plates · Free vibration · FSDT · Elastic foundation · Cut-outs · Finite element methods

S. Ghosh (✉) · S. Pal · S. Haldar
Department of Aerospace Engineering and Applied Mechanics, Indian Institute of Engineering Science and Technology, Shibpur, Howrah 711103, India
e-mail: sabyasachighos@gmail.com

1 Introduction

Various researchers have examined isotropic plates due to their widespread use in electronics, construction, and aeronautical structures. In many applications, plates are supported by an elastic foundation, such as slabs, platforms, landing strips, helipads, buildings, aircraft, spacecraft structures, and machine foundations. Dynamic analysis is conducted to ascertain how the structure responds to loads or disturbances, such as wind or earthquakes, and to determine the natural frequency to avoid resonance. Cut-out plates are utilized in numerous structural applications, such as aircraft fuselage bodies, platforms, and computer chips, and cut-outs are sometimes used to decrease the structure's mass while maintaining the plate's stiffness or to provide a passageway for movement. The dynamic behavior of plates is altered by the introduction of cut-outs. As a result, dynamic analysis of cut-out plates on elastic foundations is crucial for developing an effective design and avoiding resonance.

The vibration of isotropic plates based on the classical plate theories, first-order shear deformation theory, and higher-order shear deformation theory has been extensively researched using various analytical methods, including the Ritz method, Finite element method, and differential methods. The first plate theory, i.e., the 2D plate theory or the Classical Plate Theory (CPT) given by Kirchhoff and Love, where the effect of transverse shear deformation is neglected, establishes accurate results for the thin plates; however, neglecting the transverse shear deformation in thick plates does not yield accurate results. Effects of the transverse shear deformations were considered by Reissner, where strains are assumed to have a linear variation through the thickness of the plate, and a shear correction factor of 5/6 is used to account for the actual parabolic variation of the strain through the thickness. Kalita and Haldar (2015, 2018) employed the FSDT and considered the effects of rotary inertia to analyze the free vibration of rectangular isotropic plates. Ye et al. (2014) developed a modified Fourier solution based on the first-order shear deformation theory for the free vibration problems of moderately thick composite laminated plates with general boundary restraints and internal line supports. Haldar and Sheikh (2005) obtained the vibration response of isotropic and composite plates using the FSDT and finite element method (FEM). Nagino et al. (2008) presented the vibration analysis of rectangular isotropic plates using the FSDT and used the β-Spline Ritz method to obtain the eigen frequencies. Reddy (1984) developed a third-order higher shear deformation theory for rectangular plates. Datta and Roy (2016) developed a generalized finite element model for static and dynamic analyses of laminated composite plates using a zeroth-order shear deformation theory (ZSDT). Li et al. (2014) performed a vibration analysis of laminated composite beams using a refined higher-order shear deformation theory. Sayyad and Ghugal (2014) presented a new shear theory for isotropic, laminated composite, and sandwich plates and obtained displacements and stresses using Navier’s technique. Vu et al. (2019) presented a refined hyperbolic shear deformation theory for sandwich FG plates by enhanced meshfree with new correlation function to obtain the natural frequencies of the FGM plates and Ray (2021) derived the three-dimensional exact solutions for the static analysis of rectangular antisymmetric angle ply plates. Alsebai et al. (2022) presented a semi-analytical solution for the bending of reinforced FG Porous plates based on refined four-variable shear deformation plate theory and obtained the solutions using the Levy technique. Xue et al. (2017) performed the free vibration analysis of in-plane functionally graded plates using a refined plate theory and an Iso-geometric approach in conjunction with a refined plate theory. Qin et al. (2018) employed a nonuniform rational B-spline (NURBS) basis function to investigate the in-plane free vibration of sector, annular, and circular plates using isogeometric finite element approach. Researchers have recently utilized the Numerical Manifold Method (NMM), which is an extension of the Finite Element Method (FEM), to investigate plate and shell problems. Guo and Zheng (2017) employed the Naghdi shell model to address thin shell problems by using a high-order NMM model and effectively suppressing membrane and shear locking phenomena. Additionally, Guo et al. (2019a) utilized the NMM to conduct vibration analysis on thin plates with arbitrary shapes. Zhuang et al. (2021) proposed a deep autoencoder method and employed the minimum total potential energy principle for the bending, vibration, and buckling analysis of Kirchhoff plates. Guo et al. (2019b) proposed a deep collocation method (DCM) based on a feedforward deep neural network (DNN) for thin plate bending problems by minimizing the governing partial differential equations of the Kirchhoff plate bending problems at randomly distributed collocation points inside the plate domain.

Plates resting on point elastic support based on the Winkler elastic model were studied using a finite strip method by Huang and Thambiratnam (2001), while Lee and Lee (1997) used the Rayleigh–Ritz method. The problem of thick isotropic plates resting on the Winkler and Pasternak elastic foundation was addressed by Matsunaga (2000) using an analytical approach. Zhou et al. (2004) studied the vibration characteristic of thick rectangular plates based on the Pasternak model using the Ritz method. Xiang (2003) studied the vibration of rectangular plates based on the FSDT resting on a multi-segment Winkler-type elastic foundation using analytic methods. Zenkour et al. (2011) investigated the vibration response of rectangular orthotropic plates resting on a two-parameter (Pasternak) elastic foundation using the mixed first-order shear deformation theories, while Joodaky and Joodaky (2015) studied the vibration response of thin skew plates resting on Winkler and

Pasternak foundation model using an extended Kantorovich method (EKM). Deghan and Baradaran (2011) analyzed the vibration of a thick rectangular plate resting on a Pasternak elastic foundation using a differential quadrature method (DQM). Thai et al. (Thai et al. 2013) employed a refined shear deformation theory to obtain analytical solutions for isotropic plates on elastic foundations using a simplified FSDT. Jahromi (2013) studied the free vibration of rectangular isotropic plates based on the FSDT resting on a partial Pasternak elastic foundation using the generalized differential quadrature (GDQ) method. Zenkour (2013) studied the effects of thermo-mechanical loading on the deflection and stresses of cross-ply laminated plates resting on Pasternak elastic foundations. Atmane et al. (2010) studied the free vibration of functionally graded plates resting on Winkler–Pasternak elastic foundations using a new shear deformation theory and Navier's technique whereas, Alipour et al. (2010) described a semi analytical solution for free vibration functionally graded plates on elastic foundations. Zarouni et al. (2014) investigated the free vibration analysis of fiber-reinforced composite (FRC) conical shells resting on Pasternak-type elastic foundation and carried out a comparative study between the Ritz and Galerkin Variational methods.

Rectangular plates having cut-outs have been researched adequately, as evident by the vast literature available on the problem. Reddy (1982) investigated the vibration of composite plates with cut-outs using the finite element method based on the FSDT, while Pal et al. (2021a, b) studied the plates of the rectangular Mindlin type containing cut-outs and distributed mass using the finite element method. The effect of transverse shear deformation and rotary inertia in the vibration of rectangular plates containing cut-outs was investigated by Aksu (1984) and Lee et al. (1992). Ali and Atwal (1980) investigated the natural frequencies of rectangular plates with cut-outs using the Rayleigh method. Rajamani and Prabhakaran (1977) obtained the natural frequencies of composite plates containing cut-outs using analytical methods, while a finite strip analysis approach was employed by Ovesy and Fazilati (2012) to obtain the natural frequencies. Sun et al. (2021) employed a scaled boundary finite element method to study laminated composite plates containing multiple cut-outs. Sivakumar et al. (1999) employed the higher-order displacement theory to analyze the vibration of a laminated composite plate containing cut-outs using the Ritz finite element method. Guo et al. (2023) proposed a generalized moving least squares (GMLS) based numerical manifold method (NMM) and applied to investigate bending, vibration and buckling behaviors of thin plates with various shape and cut-outs.

While literature is available for vibration analysis of plates, plates resting on elastic foundation, and plates with cut-outs without elastic support, the novelty of this work lies in the fact that the literature study reveals a research gap in the analysis of rectangular cut-out plates resting on elastic foundation, which this work attempts to analyze. This paper attempts to study the vibration response of isotropic plates of different side-to-thickness ratios and various aspect ratios containing rectangular and square cut-outs of various sizes, resting on an elastic foundation of Winkler and Pasternak type with various stiffness coefficients based on the first-order shear deformation theory using finite element method.

The rest of the article is presented as follows, the numerical formulation is presented in the following section, followed by convergence and comparison studies with existing literature in Sect. 3, and then the parametric study of cut-out plates on elastic foundation is performed in Sect. 4 and the effect of cut-dimensions, boundary conditions, side to thickness ratios, cut-out position keeping the cut-out to edge length ratio fixed and elastic foundation stiffness parameter is investigated. Finally, a conclusion is made from the parametric study in this paper.

2 Numerical formulation

2.1 Plate constitutive equation

The relation between stress and strain can be expressed as

$$\sigma_x = \frac{E}{1-\mu^2}\left(\epsilon_x + \mu\epsilon_y\right); \quad \sigma_y = \frac{E}{1-\mu^2}\left(\epsilon_y + \mu\epsilon_x\right) \tag{1}$$

$$\begin{aligned} \tau_{xy} &= G\gamma_{xy} = \frac{E}{2(1+\mu)}\gamma_{xy}; \\ \tau_{yz} &= G\gamma_{yz} = \frac{E}{2(1+\mu)}\gamma_{yz}; \\ \tau_{xz} &= G\gamma_{xz} = \frac{E}{2(1+\mu)}\gamma_{xz} \end{aligned} \tag{2}$$

Expressing the above equation in matrix notation, $\{\sigma\} = [D]\{\epsilon\}$, where $\{\sigma\}$ is the stress vector given by $[\sigma]^T = \left[\sigma_x\ \sigma_y\ \tau_{xy}\ \tau_{yz}\ \tau_{xz}\right]$ and the strain vector $\{\varepsilon\}$ consists of $[\varepsilon]^T = \left[\epsilon_x\ \epsilon_y\ \gamma_{xy}\ \gamma_{yz}\ \gamma_{xz}\right]$.

$[D]$ is the rigidity matrix given by

$$[D] = \frac{E}{1-\mu^2}\begin{bmatrix} 1 & \mu & 0 & 0 & 0 \\ \mu & 1 & 0 & 0 & 0 \\ 0 & 0 & \frac{1-\mu}{2} & 0 & 0 \\ 0 & 0 & 0 & \frac{1-\mu}{2} & 0 \\ 0 & 0 & 0 & 0 & \frac{1-\mu}{2} \end{bmatrix} \tag{3}$$

2.1.1 Plate displacement field

The total rotation of the transverse normal about y-axis ($\varnothing_x$) include rotation due to bending given by $\left(\theta_x\right)$ in the *xz*-plane, and the rotation due to shearing along the thickness of the plate is $\left(\psi_{xz}\right)$. Therefore, the total rotation of the transverse normal in the *xz*- plane is given by

$$\emptyset_x = \psi_{xz} + \theta_x \tag{4}$$

Further, the rotation due to bending in the xz-plane about the y-axis is given by

$$\theta_x = \frac{\partial w}{\partial x} \tag{5}$$

The plate deformation is given by

$$\begin{aligned} u(x,y,z,t) &= u_0(x,y,z) - z\emptyset_x(x,y,t), v(x,y,z,t) \\ &= v_0(x,y,z) - z\emptyset_y(x,y,t), w(x,y,z,t) = w(x,y,t) \end{aligned} \tag{6}$$

The generalized strain matrix can be represented in the matrix form given as

$$\begin{Bmatrix} \epsilon_x \\ \epsilon_y \\ \gamma_{xy} \\ \gamma_{xz} \\ \gamma_{yz} \end{Bmatrix} = \begin{Bmatrix} \frac{\partial u}{\partial x} \\ \frac{\partial v}{\partial y} \\ \left(\frac{\partial u}{\partial y} + \frac{\partial v}{\partial x}\right) \\ \emptyset_x - \frac{\partial w}{\partial x} \\ \emptyset_y - \frac{\partial w}{\partial y} \end{Bmatrix} = \begin{Bmatrix} z\frac{\partial \emptyset_x}{\partial x} \\ z\frac{\partial \emptyset_y}{\partial y} \\ z\left(\frac{\partial \emptyset_x}{\partial y} + \frac{\partial \emptyset_y}{\partial x}\right) \\ \emptyset_x - \frac{\partial w}{\partial x} \\ \emptyset_y - \frac{\partial w}{\partial y} \end{Bmatrix} \tag{7}$$

The moments M_x, M_y, M_{xy} is given by

$$\begin{Bmatrix} M_x \\ M_y \\ M_{xy} \end{Bmatrix} = \int_{-h/2}^{+h/2} \begin{Bmatrix} \sigma_x \\ \sigma_y \\ \tau_{xy} \end{Bmatrix} z.dz \tag{8}$$

2.1.2 Transverse shear forces

$$\begin{Bmatrix} Q_x \\ Q_y \end{Bmatrix} = \boldsymbol{\kappa} \int_{-h/2}^{+h/2} \begin{Bmatrix} \tau_{xz} \\ \tau_{yz} \end{Bmatrix} dz \tag{9}$$

where $\boldsymbol{\kappa}$ is the shear correction factor taken as 5/6 to account for the parabolic variation of shear strain through the thickness of the plate as compared to linear variation assumed in the first-order shear deformation theory.

Integrating and assembling the moments and transverse shear forces from Eqs. (8) and (9), the expression given in Eq. (10) is obtained.

$$\begin{Bmatrix} M_x \\ M_y \\ M_{xy} \\ Q_x \\ Q_y \end{Bmatrix} = \begin{bmatrix} D_{44} & D_{45} & 0 & 0 & 0 \\ D_{54} & D_{55} & 0 & 0 & 0 \\ 0 & 0 & D_{66} & 0 & 0 \\ 0 & 0 & 0 & Q_{77} & 0 \\ 0 & 0 & 0 & 0 & Q_{88} \end{bmatrix} \begin{Bmatrix} \frac{\partial \emptyset_x}{\partial x} \\ \frac{\partial \emptyset_y}{\partial y} \\ \left(\frac{\partial \emptyset_x}{\partial y} + \frac{\partial \emptyset_y}{\partial x}\right) \\ \frac{\partial w}{\partial x} + \emptyset_x \\ \frac{\partial w}{\partial y} + \emptyset_y \end{Bmatrix} \tag{10}$$

$$\begin{aligned} &D_{44} = D_{55} = \frac{Eh^3}{12\left(1-\mu^2\right)};\quad D_{45} = D_{54} = \frac{\mu E h^3}{12\left(1-\mu^2\right)}; \\ &D_{66} = \frac{Eh^3}{24(1+\mu)} = \frac{Gh}{12};\quad Q_{77} = Q_{88} = \frac{\kappa E h}{2(1+\mu)} = \boldsymbol{\kappa} G h \end{aligned} \tag{11}$$

2.2 Finite element formulation

A 9- *noded five d.o.f* isoparametric plate bending element is used to formulate the plate equation.

The coordinate within an element is given by

$$x = N_r x_r, y = N_r y_r \tag{12}$$

where x_r and y_r are in the nodal coordinates and x and y are in the cartesian coordinates.

N_r is the shape function of the *r*th node in the above expression, which is also used to represent the displacement fields in the element.

Shear locking is an unavoidable phenomenon noticed in plate bending element problems. To avoid this, various techniques such as reduced integration techniques in evaluating the shear energy term or mixed interpolation approach in which the shear terms are first approximated independently and then eliminated from the system as demonstrated by Iosilevich et al. (1997) is used to formulate the plate bending problem. In this study isoparametric element interpolation technique is used to formulate the transverse displacements and section rotations in the elements, and the reduced integration technique using a 2×2 gauss point has been implemented in the formulation to avoid the shear locking phenomenon.

The Lagrangean interpolation gives the 9-shape function as per the following expression.

$$\begin{aligned} &N_1 = \frac{\xi\eta}{4}(\xi-1)(\eta-1); \quad N_2 = \frac{\xi\eta}{4}(\xi+1)(\eta-1); \quad N_3 = \frac{\xi\eta}{4}(\xi+1)(\eta+1) \\ &N_4 = \frac{\xi\eta}{4}(\xi-1)(\eta+1); \quad N_5 = \frac{\eta}{2}\left(1-\xi^2\right)(\eta-1); \quad N_6 = \frac{\xi}{2}(\xi+1)\left(1-\eta^2\right) \\ &N_7 = \frac{\eta}{2}\left(1-\xi^2\right)(1+\eta); \quad N_8 = \frac{\xi}{2}(\xi-1)\left(1-\eta^2\right); \quad N_9 = \left(1-\xi^2\right)\left(1-\eta^2\right) \end{aligned} \tag{13}$$

Each node has five degrees of freedom, two in-plane displacements (u,v), one transverse (w), and two rotational ($\varnothing_x$) and ($\varnothing_y$).

The nodal displacement vector is given by

$$\{\delta\}_r = \sum_{r=1}^{r=9} \begin{Bmatrix} u_r \\ v_r \\ w_r \\ \varnothing_{xr} \\ \varnothing_{yr} \end{Bmatrix}_{45\times 1} \tag{14}$$

The nodal displacement can be mapped to the element displacement in terms of shape function using the relation:

$$\{\delta\} = \sum_{r=1}^{9} [N]_r \{\delta\}_r \tag{15}$$

The strain vector is expressed in terms of nodal displacement and shape function given by the expression

$$\{\boldsymbol{\epsilon}\} = [\boldsymbol{B}]\{\boldsymbol{\delta}\}_r \tag{16}$$

where $[\boldsymbol{B}]$ is the strain displacement matrix, and it is expressed as

$$[\boldsymbol{B}] = \begin{bmatrix} \frac{\partial N_r}{\partial x} & 0 & 0 & \frac{\partial N_r}{\partial x} & 0 \\ 0 & \frac{\partial N_r}{\partial y} & 0 & 0 & \frac{\partial N_r}{\partial y} \\ \frac{\partial N_r}{\partial y} & \frac{\partial N_r}{\partial x} & 0 & \frac{\partial N_r}{\partial y} & \frac{\partial N_r}{\partial x} \\ 0 & 0 & \frac{\partial N_r}{\partial x} & -N_r & 0 \\ 0 & 0 & \frac{\partial N_r}{\partial y} & 0 & -N_r \end{bmatrix}$$

2.3 Equation of motion

The total energy Π is the summation of Π_{p} = Strain Energy of Plate, Π_{ef} = Strain Energy of Elastic Foundation, Π_{ke} = Kinetic Energy of Plate.

The principle of minimum virtual energy states that

$$0 = \int_0^T \left(\delta\Pi_{\mathrm{p}} + \delta\Pi_{ef} - \delta\Pi_{ke}\right) dt \tag{17}$$

The strain energy of the plate is given by

$$\Pi_{\mathrm{p}} = \frac{1}{2} \int_A \int_{-\frac{h}{2}}^{\frac{h}{2}} \left[\sigma_x \epsilon_x + \sigma_y \epsilon_y + \tau_{xy}\gamma_{xy} + \tau_{xz}\gamma_{xz} + \tau_{yz}\gamma_{yz}\right] dz dA \tag{18}$$

The energy stored in the plate in matrix form

$$\Pi_{\mathrm{p}} = \frac{1}{2} \int_V \{\sigma\}^T \{\varepsilon\} dV \tag{19}$$

$$\{\sigma\}^T = [\varepsilon]^T [D] \tag{20}$$

$$\Pi_{\mathrm{p}} = \frac{1}{2} \int_V [\varepsilon]^T [D] \{\varepsilon\} dV = \frac{1}{2} \int_V [\delta]_r^T [B]^T [D][B][\delta]_r dV \tag{21}$$

$$\frac{\delta\Pi_{\mathrm{p}}}{\delta\delta} = \int_0^b \int_0^a [B]^T[D][B]dxdy \tag{22}$$

$$\left[\boldsymbol{K_{ij}}\right]_p = \int_{-1}^{+1} \int_{-1}^{+1} [B]^T[D][B]|J|d\xi d\eta \tag{23}$$

2.3.1 Winkler and Pasternak elastic foundation model

The load–deflection equation in the Winkler and Pasternak elastic foundation model is given by:

$$P = k_0 w(x,y) - k_S\left(\frac{\partial^2 w(x,y)}{\partial x^2} + \frac{\partial^2 w(x,y)}{\partial y^2}\right) \tag{24}$$

K_0 is the Winkler stiffness coefficient which takes into account only the transverse deflection of the springs, and K_S is the Pasternak stiffness coefficient which accounts for the shearing effects of the springs; setting the Pasternak stiffness coefficient to zero effectively reduces the elastic foundation model to Winkler model, i.e., if K_S is equal to zero, the elastic foundation model reduces to a Winkler model.

The strain energy due to the elastic foundation is given by:

$$\begin{aligned}\Pi_{\mathrm{ef}} &= \frac{1}{2}\int_A \left(\left[w(x,y)\right]^T k_0 \left[w(x,y)\right]\right)dA \\ &\quad + \frac{1}{2}\int_A \left(\left[\frac{\partial w}{\partial x}, \frac{\partial w}{\partial y}\right]^T k_S \left[\frac{\partial w}{\partial x}, \frac{\partial w}{\partial y}\right]\right)dA\end{aligned} \tag{25}$$

The first term of the right side of Eq. (25) in the equation represents the strain energy due to the Winkler foundation Π_{ef1} and the second term represents the strain energy due to the Pasternak foundation Π_{ef2}

$$\Pi_{\mathrm{ef}} = \Pi_{\mathrm{ef1}} + \Pi_{\mathrm{ef2}}$$

Minimizing the terms in Eq. (25) individually w.r.t the transverse deflections, the stiffness matrix can be obtained as described.

$$\frac{\delta^2\Pi_{\mathrm{ef1}}}{\delta w_i \delta w_j} = \frac{1}{2}k_0 \frac{\delta^2}{\delta w_i \delta w_j}\int_0^b \int_0^a \left[w(x,y)\right]^T\left[w(x,y)\right]dxdy \tag{26}$$

$$\left[\boldsymbol{K_{ij}}\right]_0 = k_0 \int_{-1}^{+1}\int_{-1}^{+1} \left[N_i\right]^T\left[N_j\right]|J|d\xi d\eta \tag{27}$$

$$\frac{\delta^2\Pi_{\mathrm{ef2}}}{\delta w_i \delta w_j} = \frac{1}{2}\left(k_S\right)\frac{\delta^2}{\delta w_i \delta w_j}\int_0^b \int_0^a \left[\frac{\partial w}{\partial x}, \frac{\partial w}{\partial y}\right]^T\left[\frac{\partial w}{\partial x}, \frac{\partial w}{\partial y}\right]dxdy \tag{28}$$

Substituting w(x,y) in terms of shape function N_r and integrating the expression

$$\begin{aligned}\left[\boldsymbol{K_{ij}}\right]_S = k_S \int_{-1}^{+1}\int_{-1}^{+1} &\left(\frac{1}{a^2}\left[\frac{\partial N_i}{\partial \xi}\right]^T\left[\frac{\partial N_j}{\partial \xi}\right]\right. \\ &\left.+\frac{1}{b^2}\left[\frac{\partial N_i}{\partial \eta}\right]^T\left[\frac{\partial N_j}{\partial \eta}\right]\right)|J|d\xi d\eta\end{aligned} \tag{29}$$

The total stiffness of the plate is written as

$$\left[\boldsymbol{K_{ij}}\right] = \left[\boldsymbol{K_{ij}}\right]_p + \left[\boldsymbol{K_{ij}}\right]_0 + \left[\boldsymbol{K_{ij}}\right]_S \tag{30}$$

The kinetic energy of the plate is given as:

$$\Pi_{ke} = \frac{1}{2}\int_A \int_{-\frac{h}{2}}^{+\frac{h}{2}} \rho\left\{\dot{u}^2 + \dot{v}^2 + \dot{w}^2\right\}dzdA \tag{31}$$

$$\begin{aligned}\delta\Pi_{ke} = \int_A \int_{-\frac{h}{2}}^{+\frac{h}{2}} &\rho\left\{\left(\dot{u}_0 + z\dot{\phi}_x\right)\left(\delta\dot{u}_0 + z\delta\dot{\phi}_x\right)\right. \\ &\left.+\left(\dot{v}_0 + z\dot{\phi}_y\right)\left(\delta\dot{v}_0 + z\delta\dot{\phi}_y\right) + \left(\dot{w}_0\delta\dot{w}_0\right)\right\}dzdA\end{aligned} \tag{32}$$

$$\begin{aligned}\delta\Pi_{ke} = \rho\int_A &\left\{\mathrm{I}_0\left(\dot{u}_0\delta\dot{u}_0 + \dot{v}_0\delta\dot{v}_0 + \dot{w}_0\delta\dot{w}_0\right)\right. \\ &+\mathrm{I}_1\left(\dot{\phi}_x\delta\dot{u}_0 + \dot{u}_0\delta\dot{\phi}_x + \dot{\phi}_x\delta\dot{v}_0 + \delta\dot{\phi}_y\dot{v}_0\right)\} \\ &\left.+\mathrm{I}_2\left(\dot{\phi}_x\delta\dot{\phi}_x + \dot{\phi}_y\delta\dot{\phi}_y\right)dA\right\}\end{aligned} \tag{33}$$

$$\begin{Bmatrix} I_0 \\ I_1 \\ I_2 \end{Bmatrix} = \int_{-h/2}^{+h/2} \begin{Bmatrix} 1 \\ z \\ z^2 \end{Bmatrix} dz = \begin{Bmatrix} h \\ 0 \\ \frac{h^3}{12} \end{Bmatrix} \tag{34}$$

The I_2 terms account for the plate's rotary inertia, which becomes significant as the plate thickness ratio increases.

The consistent mass matrix of the element is given by

$$[\boldsymbol{M}]^c = \rho \int_{-1}^{+1}\int_{-1}^{+1} \left\{ I_0 \left\{ [N_u]^T[N_u] + [N_v]^T[N_v] + [N_w]^T[N_w] \right\} + I_2 \left\{ [N_{\phi_x}]^T[N_{\phi_x}] + [N_{\phi_y}]^T[N_{\phi_y}] \right\} \right\} |J| d\xi d\eta \tag{35}$$

where

$$[N_u] = [\,[N_r]\ [N_0]\ [N_0]\ [N_0]\ [N_0]\,]$$

$$[N_v] = [\,[N_0]\ [N_r]\ [N_0]\ [N_0]\ [N_0]\,]$$

$$[N_w] = [\,[N_0]\ [N_0]\ [N_r]\ [N_0]\ [N_0]\,]$$

$$[N_{\emptyset_x}] = [\,[N_0]\ [N_0]\ [N_0]\ [N_r]\ [N_0]\,]$$

$$[N_{\emptyset_y}] = [\,[N_0]\ [N_0]\ [N_0]\ [N_0]\ [N_r]\,]$$

$[N_0]$ is a null matrix of order 1×9.

The lumped mass matrix $[M]$ is derived from the consistent mass matrix using a mass lumping scheme described by Haldar (2008). The lumped mass matrix is a diagonal matrix of order 45×45 with the non-zero diagonal elements corresponding to the u, v, w, ϕ_x, ϕ_y. The distribution of the lumped mass at the degree of freedom has been made in proportion to the diagonal element of the consistent mass matrix of Eq. (35) as follows:

$$m_{ii}^{ul} = I_0 \frac{m_{ii}}{\sum m_{ii}} m_e (i = 1, 6, 11, 16, 21, 26, 31, 36, 41)$$

$$m_{ii}^{vl} = \mathrm{I}_0 \frac{m_{ii}}{\sum m_{ii}} m_e (i = 2, 7, 12, 17, 22, 27, 32, 37, 42)$$

$$m_{ii}^{wl} = \mathrm{I}_0 \frac{m_{ii}}{\sum m_{ii}} m_e (i = 3, 8, 13, 18, 23, 28, 33, 38, 43)$$

$$m_{ii}^{\phi_x l} = \mathrm{I}_2 \frac{m_{ii}}{\sum m_{ii}} m_e (i = 4, 9, 14, 19, 24, 29, 34, 39, 44)$$

$$m_{ii}^{\phi_y l} = \mathrm{I}_2 \frac{m_{ii}}{\sum m_{ii}} m_e (i = 5, 10, 15, 20, 25, 30, 35, 40, 45)$$

where m_e is the mass of the element and m_{ii} is the ith diagonal element of the consistent mass matrix and $m_{ii}^{ul}, m_{ii}^{vl}, m_{ii}^{wl}, m_{ii}^{\phi_x l}, m_{ii}^{\phi_y l}$ are the ith diagonal element corresponding to u, v, w, ϕ_x, ϕ_y of the lumped mass matrix.

The global stiffness matrix $[K_G]$ and the global mass matrix $[M_G]$ is obtained for the plate after assembling the individual element stiffness matrices $[K_{ij}]$ and the lumped mass matrices $[M_{ii}]$ obtained over the entire region of the plate.

Finally, substituting Eqs. (14), (30) and (35) into Eq. (17), we arrive at the equation of the motion, where $\boldsymbol{\omega}$ is the frequency of the vibration response

$$\left\{ [\boldsymbol{K_G}] - \boldsymbol{\omega}^2 [\boldsymbol{M_G}] \right\} \{\boldsymbol{\delta}\}_{\boldsymbol{r}} = 0 \tag{36}$$

The Natural Frequency $\boldsymbol{\omega}$ and the Winkler stiffness $\boldsymbol{K}_0$ and Pasternak stiffness $\boldsymbol{K_S}$ are expressed in the non-dimension using the following relations.

$$\overline{\boldsymbol{\omega}} = \boldsymbol{\omega a}^2 \sqrt{\frac{\boldsymbol{\rho h}}{\boldsymbol{D}}}; \quad \overline{\boldsymbol{K}_0} = \frac{\boldsymbol{K}_0 \boldsymbol{a}^4}{\boldsymbol{D}}; \quad \overline{\boldsymbol{K_S}} = \frac{\boldsymbol{K_S a}^2}{\boldsymbol{D}} \tag{37}$$

In the present formulation, the boundary conditions are described using the degrees of freedom of the plate element.

Simple Support :	$\mathrm{v, w}, \emptyset_y = 0$	at $\mathrm{x} = 0,\ \mathrm{a}$
	$\mathrm{u, w}, \emptyset_x = 0$	at $\mathrm{y} = 0,\ \mathrm{b}$
Clamped :	$\mathrm{u, v, w}, \emptyset_x, \emptyset_y = 0$	at $\mathrm{x} = 0,\ \mathrm{a};\ \mathrm{y} = 0,\ \mathrm{b}$

The boundary condition (B.C) in this paper has been described using a 4-letter notation. For example, if the B.C is described as SCSF, it can be interpreted that in Fig. 1, the left edge and the right edge (x = 0, a) are simply supported and clamped, respectively, and the bottom edge and the top edge (y = 0, b) are simply supported and free respectively (Fig. 2).

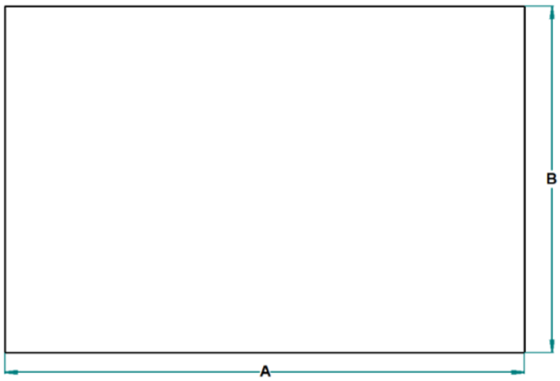

Fig. 1 Rectangular plate with aspect ratio a/b resting on elastic foundation

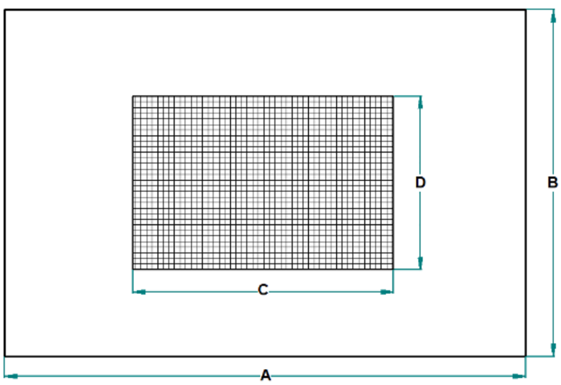

Fig. 2 Rectangular plate of aspect ratio a/b containing a central rectangular cut-out of aspect ratio of c/d resting on an elastic foundation

3 Convergence and validation

To illustrate the robustness and ascertain the accuracy of the current formulation, various plates with different boundary conditions and elastic foundations are analyzed and compared with the established results. New results are obtained for plates resting on elastic foundations with different cut-outs and thickness-to-side ratios having different boundary conditions and elastic foundation stiffness parameters.

3.1 Convergence and effect of rotary inertia on the natural frequency of thick and thin plates

The free vibration of plates resting on elastic foundations with various stiffness parameters and different boundary conditions is analyzed for plates having various thickness-to-side ratios.

The fundamental frequencies are obtained using various mesh divisions N_M, and the results are obtained both without consideration of rotary inertia (WORI) and with the consideration of rotary inertia (WRI) in Fig. 3. The results obtained are compared with the established results given by Akhavan et al. (2009) in which the FSDT was employed to obtain the exact solutions of plates resting on elastic foundation. The figure shows that the present formulation predicts accurate results for both thick and thin plates with various boundary conditions at around 18×18 mesh divisions.

It can be seen that the effect of rotary inertia is negligible for thin plates, whereas, for thick plates inclusion of rotary inertia establishes accurate results. Therefore, to obtain different results, the effect of rotary inertia will be considered in both thick and thin plates to predict the fundamental frequencies accurately, and the results are obtained using 20×20 mesh divisions.

3.2 Natural frequencies of thin plates resting on elastic foundation

A thin square plate resting on an elastic foundation with varying Winkler stiffness parameter K_0 and Pasternak stiffness parameter K_S is considered. The first three natural frequencies of a plate clamped on all edges and having a thickness-to-side ratio of 0.015 are obtained in Table 1, and the results are compared with that of existing results obtained by Jahromi et al. (2013), and it can be observed that the first three natural frequencies are predicted accurately using the present formulation, for a plate clamped on all edges resting on elastic foundation.

3.3 Effect of increasing elastic foundation stiffness parameters

Square plates with simply supported boundary conditions on all edges and resting on an elastic foundation of various stiffness parameters and with thickness-to-side ratios of 0.05 (Thin), 0.1 (Moderately Thick), and 0.2 (Thick) is considered. The fundamental frequencies obtained by varying the

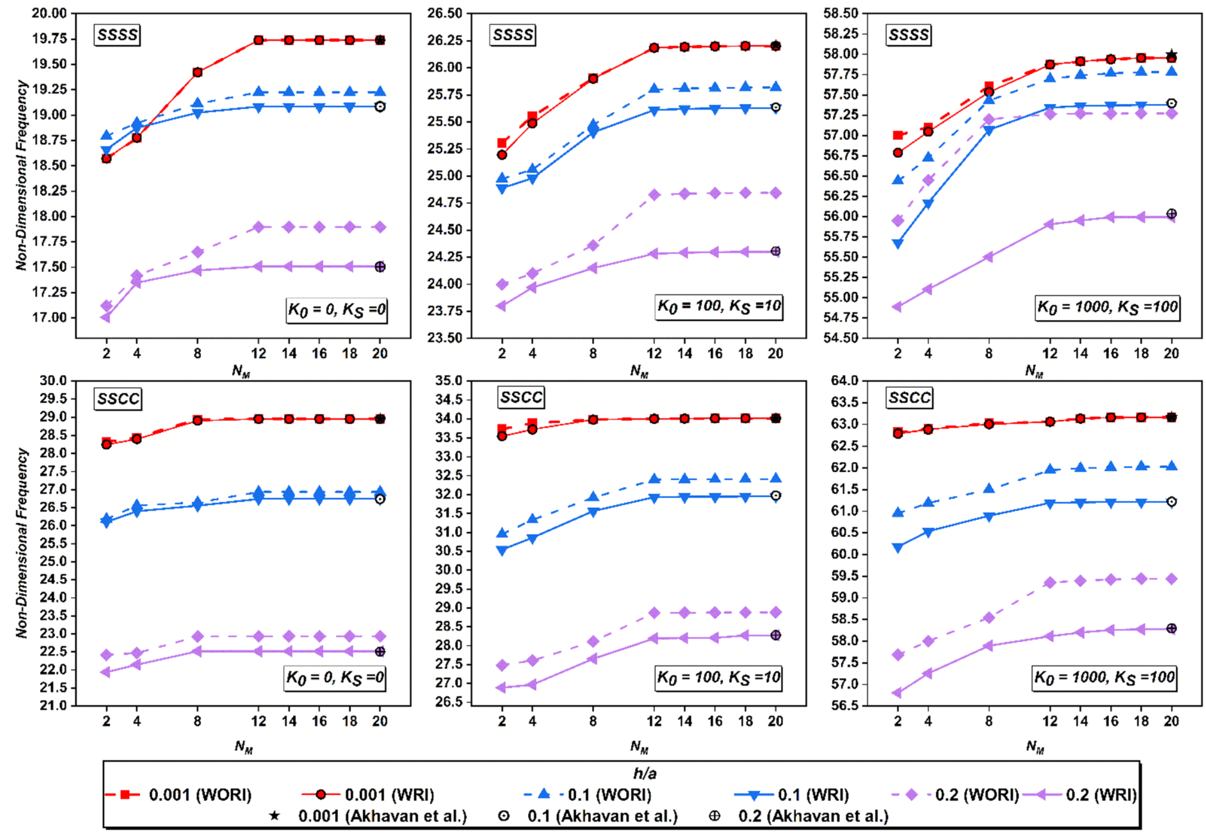

Fig. 3 Fundamental frequency for a square isotropic plate without and with elastic foundation, with varying thickness-to-side ratio for SSSS and SSCC boundary condition obtained at different mesh divisions N_M, along with established results obtained by Akhavan et al.

Table 1 Non-dimensional frequency parameter of a clamped square isotropic having a thickness-to-side ratio of 0.015 and varying stiffness parameter

K_0	K_S	Formulation	Frequency parameter		
			ω_1	ω_2	ω_3
1390.2	0	Jahromi et al. (2013)	5.244	8.314	11.538
		Present	5.243	8.308	11.525
	166.83	Jahromi et al. (2013)	8.167	12.823	16.833
		Present	8.128	12.795	16.736
2780.4	0	Jahromi et al. (2013)	6.463	9.131	12.139
		Present	6.462	9.131	12.138

elastic stiffness parameters are plotted in Fig. 4 for plates of different thickness ratios. It can be observed that after specific Winkler and Pasternak stiffness parameters for a particular thickness-to-side ratio, any increment in stiffness produces no further change in the non-dimensional frequency obtained for the plate, which indicates that the plate has maximum stiffness at the particular thickness ratio and any further increment of elastic foundation stiffness does not affect the stiffness of the plate.

3.4 Effect of aspect ratio, thickness-to-side ratio, and elastic foundation parameter

An isotropic plate clamped on edges and resting on an elastic foundation with various Winkler and Pasternak elastic foundation stiffness parameters is considered, and the frequencies are obtained for a plate with aspect ratios (a/b) of 0.5, 1.0, and 2.0 and thickness-to-side ratios of 0.01, 0.10 and 0.20. The present results in Table 2 are compared with the existing results obtained using a refined shear

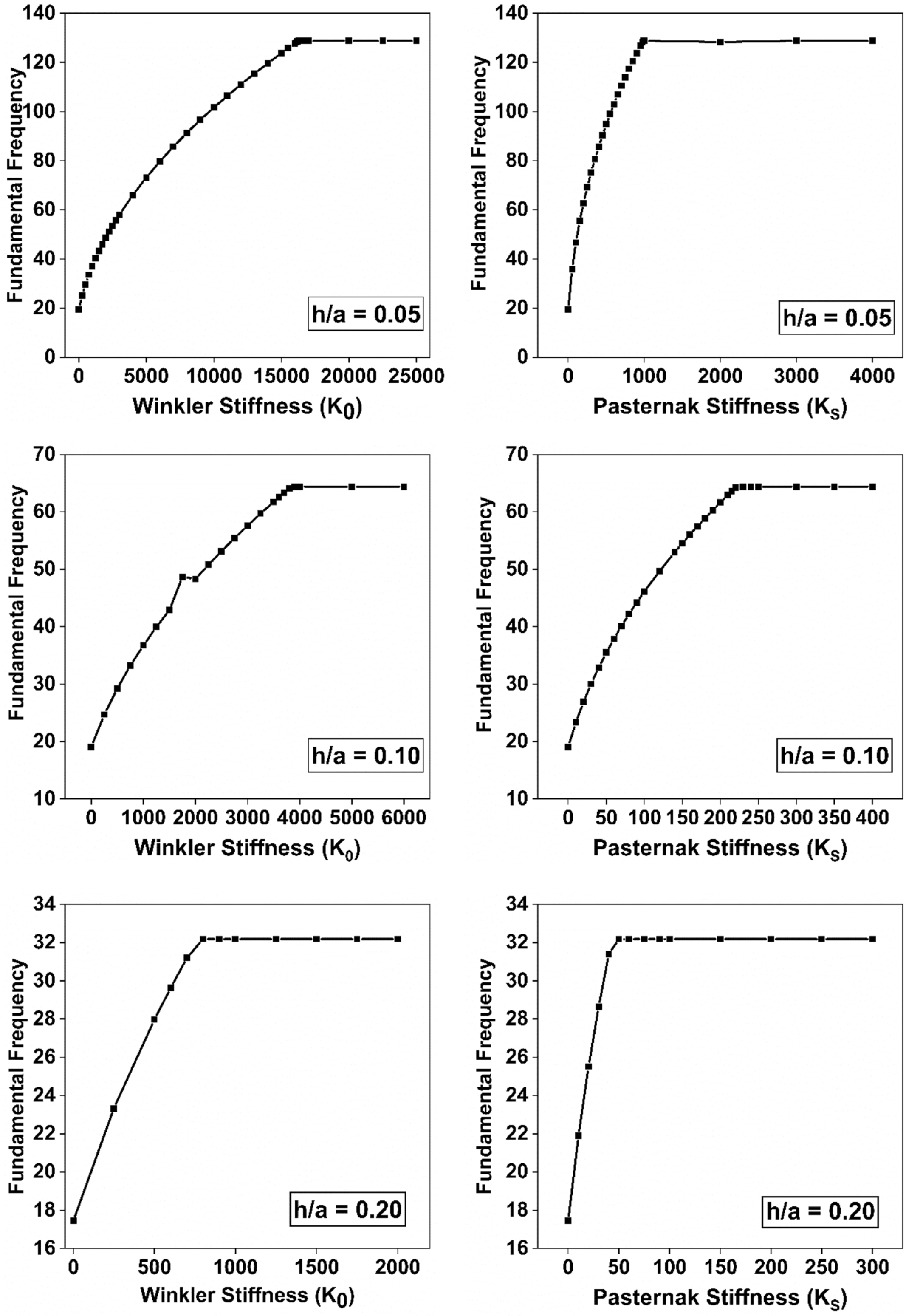

Fig. 4 Fundamental Frequency of a square plate having various thickness-to-side ratios and the vibration response with increasing stiffness parameters

Table 2 Non-dimensional frequency of simply supported isotropic plate with varying aspect ratio and various thickness-to-side ratios resting on elastic foundation with various stiffness parameters

K_0, K_S	a/b	h/b	Method	ω_1	ω_2	ω_3	ω_4	ω_5	ω_6
10, 10	0.5	0.2	Thai et al. (2013)	16.079	22.429	32.000	38.979	43.901	51.611
			Present	15.845	22.047	31.878	38.281	43.562	51.391
		0.1	Thai et al. (2013)	16.665	23.830	35.289	44.118	50.567	61.019
			Present	16.053	23.430	35.085	43.378	50.359	60.668
		0.01	Thai et al. (2013)	16.896	24.428	36.856	46.755	54.167	66.505
			Present	16.287	24.009	36.578	45.915	53.981	65.909
	1.0	0.2	Thai et al. (2013)	22.429	43.901	61.562	71.984	86.165	103.062
			Present	22.047	43.401	61.660	71.810	86.057	102.894
		0.1	Thai et al. (2013)	23.830	50.567	75.091	90.466	112.305	139.503
			Present	23.431	50.558	75.014	90.211	112.137	139.253
		0.01	Thai et al. (2013)	24.428	54.167	83.756	103.449	132.952	172.232
			Present	24.009	53.979	83.283	103.360	132.322	172.096
	2.0	0.2	Thai et al. (2013)	43.900	61.562	86.164	103.062	114.600	132.205
			Present	43.759	61.459	86.065	102.987	114.286	132.075
		0.1	Thai et al. (2013)	50.565	75.090	112.090	139.502	158.690	188.750
			Present	50.557	75.013	111.966	139.462	158.440	188.373
		0.01	Thai et al. (2013)	54.167	83.756	132.952	172.232	201.651	250.608
			Present	53.980	83.283	132.322	172.100	201.477	250.300
100, 10	0.5	0.2	Thai et al. (2013)	18.594	24.272	33.299	40.044	44.845	52.412
			Present	18.342	24.014	33.177	39.953	44.596	52.186
		0.1	Thai et al. (2013)	19.154	25.623	36.515	45.099	51.422	61.725
			Present	18.997	25.249	36.315	44.881	51.412	61.473
		0.01	Thai et al. (2013)	19.377	26.205	38.057	47.708	54.991	67.178
			Present	19.144	25.912	37.859	47.478	54.270	66.883
	1.0	0.2	Thai et al. (2013)	24.272	44.845	62.231	72.555	86.641	103.461
			Present	23.914	44.345	62.196	72.470	86.204	103.198
		0.1	Thai et al. (2013)	25.623	51.422	75.662	90.937	112.682	139.804
			Present	25.249	51.411	75.581	90.676	112.607	139.346
		0.01	Thai et al. (2013)	26.205	54.991	84.292	103.883	133.290	172.492
			Present	26.012	54.470	83.977	103.278	132.859	172.194
	2.0	0.2	Thai et al. (2013)	44.845	62.231	86.641	103.461	114.959	132.517
			Present	44.994	62.319	86.929	103.979	114.986	132.957
		0.1	Thai et al. (2013)	51.422	75.662	112.682	139.804	158.954	188.970
			Present	51.411	75.580	112.607	139.688	158.895	188.822
		0.01	Thai et al. (2013)	54.991	84.292	133.290	172.492	201.873	250.788
			Present	54.805	83.975	133.065	172.460	201.510	250.477

deformation theory (RSDT) in which the shear correction factor is not required and contains two unknown variables by Thai et al. (2013). Table 2 presents the first six natural frequencies, where it can be observed that the present result stands in good agreement with the established results.

3.5 Simply supported isotropic square plate containing cut-outs of various thickness ratios

Simply supported isotropic square plates containing square central cut-outs as given in Fig. 2, of various cut-out size (c/a ratio), is considered. The non-dimensional frequency is obtained for various thickness-to-side ratios and a cut-out to plate edge

Table 3 Fundamental frequency of a square isotropic plate with varying side to thickness ratio and having square central cut-out with c/a = 0.5

a/h	5	10	20	25	100
Present	21.345	22.628	23.106	23.185	23.393
SP-FSM (Ovesy and Fazilati 2012)	20.168	22.338	23.143	23.265	23.574
Diff. (%)	**5.836**	**1.298**	**0.160**	**0.344**	**0.768**
FEM (Reddy 1982)	21.554	22.804	23.240	23.309	23.489
Diff. (%)	**0.970**	**0.772**	**0.577**	**0.532**	**0.409**

length (c/a) ratio of 0.5 in Table 3, where the results are compared with the results given by Ovesy and Fazilati (2012), who obtained the results using a Finite Strip Method (FSM) and the results obtained by Reddy (1982) using the Finite Element Method (FEM). Also, the effect of increasing cut-out size in a simply supported plate is investigated in Table 4, where the cut-out size is gradually increased from a c/a ratio of 0 (no cut-out) to a c/a ratio of 0.8 for various thickness ratios.

The percentage difference between the results obtained using the present method and the results obtained in the established literature are given in Tables 3 and 4 in bold and it can be observed that the present formulation accurately establishes the non-dimensional frequency of an isotropic plate containing cut-outs and stands in very close agreement with the results obtained using the Finite Element Method.

4 New results

After sufficient validation, it is clear that the present formulation accurately predicts the natural frequency of plates having different boundary conditions and thickness ratios with different elastic stiffness parameters. It also predicts the frequency of plates containing cut-outs accurately. To the authors' knowledge, there are no existing results on the dynamic analysis of cut-out plates resting on an elastic foundation, and therefore, no comparison studies could be performed for cut-out plates on an elastic foundation. The present formulation is applied to analyze the cut-outs plates resting on an elastic foundation, and parametric studies are performed in this section.

4.1 Square isotropic plate with and without elastic foundation

The first four mode shapes of a simply supported square plate having a thickness-to-side ratio (h/a) of 0.15 are presented in Fig. 5 for two types of plate, one without an elastic foundation and one resting on an elastic foundation having a stiffness parameter of $K_0 = 5000$ and $K_S = 750$. The fundamental frequencies are given above the respective mode shapes, and it can be observed that introducing an elastic foundation increases the frequency of the vibration of the plates and reduces the peak deflection at the respective modes of vibration. This finding is concurrent with the expected outcome of introducing an elastic foundation to a simply supported plate.

4.2 Square isotropic plate with a cut-out of various thickness ratios resting on elastic foundation

The first six natural frequencies of a simply supported square plate are obtained for a plate having varying thickness-to-side ratios, and the results are obtained for two types of plate, one without any cut-out

Table 4 Fundamental frequency parameter for a simply supported square isotropic plate having central square cut-outs of varying size and different side to thickness ratio and no elastic foundation

c/a	a/h = 5			a/h = 10			a/h = 1000		
	Present	JN Reddy (1982)	Diff. (%)	Present	JN Reddy (1982)	Diff. (%)	Present	JN Reddy (1982)	Diff. (%)
0	17.442	17.458	**0.092**	19.059	19.077	**0.094**	19.734	19.752	**0.091**
0.2	17.424	17.452	**0.160**	18.563	18.679	**0.621**	19.119	19.200	**0.422**
0.4	18.998	19.163	**0.861**	20.100	20.246	**0.721**	20.740	20.807	**0.322**
0.5	21.332	21.554	**1.030**	22.614	22.804	**0.833**	23.438	23.515	**0.327**
0.6	25.347	25.688	**1.327**	27.102	27.379	**1.012**	28.354	28.453	**0.348**
0.8	43.506	44.069	**1.278**	50.989	51.465	**0.925**	57.371	57.512	**0.245**

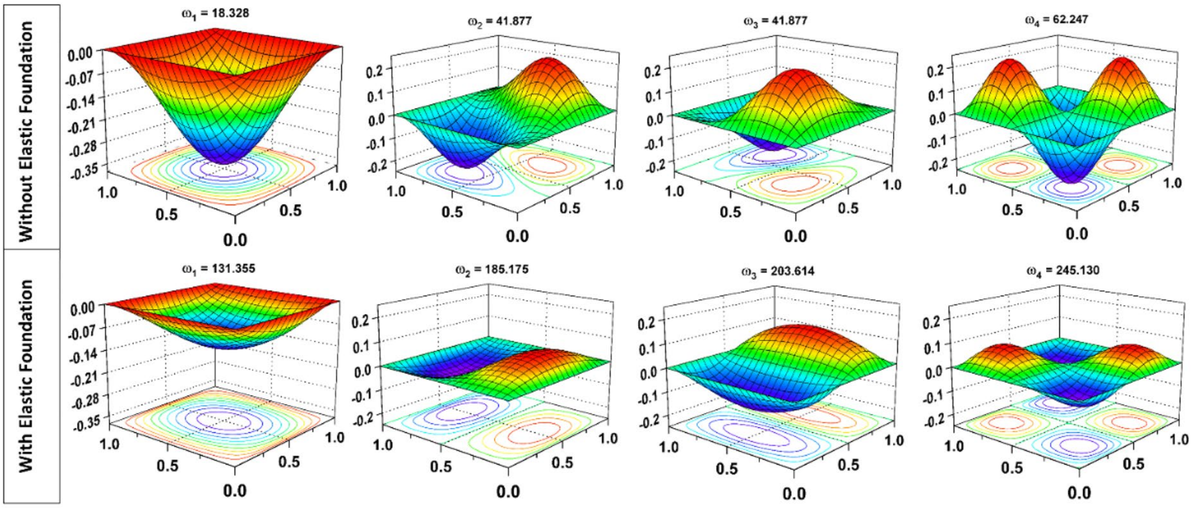

Fig. 5 First four mode shapes of the natural vibration, with and without elastic foundation

Table 5 Non-dimensional frequencies of a square isotropic plate with and without cut-outs with varying thickness-to-side ratio and different elastic stiffness parameters

h/a	c/a	K_0, K_S	ω_1	ω_2	ω_3	ω_4	ω_5	ω_6
0.01	0	0, 0	19.732	49.304	49.304	78.842	98.521	98.521
		1000, 100	55.843	86.387	90.113	119.151	136.840	142.557
	0.4	0, 0	20.708	40.719	40.719	71.166	81.631	117.131
		1000, 100	67.452	78.956	83.418	112.245	117.775	156.796
0.05	0	0, 0	19.562	48.270	48.270	76.259	94.549	94.549
		1000, 100	55.595	85.320	89.202	116.822	133.184	139.160
	0.4	0, 0	20.416	38.873	38.873	68.750	75.755	109.955
		1000, 100	66.892	77.545	82.226	110.163	113.313	150.573
0.10	0	0, 0	19.065	45.483	45.483	69.795	85.040	85.041
		1000, 100	54.880	82.492	86.838	111.199	123.155	123.156
	0.4	0, 0	19.813	35.870	35.870	63.205	66.209	96.077
		1000, 100	65.319	74.588	79.883	105.263	106.134	138.796
0.20	0	0, 0	17.449	38.153	38.152	55.150	61.578	61.578
		1000, 100	52.610	61.578	61.578	73.354	75.206	81.049
	0.4	0, 0	18.103	29.525	29.526	49.143	50.623	70.722
		1000, 100	60.438	67.196	74.241	75.863	78.076	78.077

(c/a = 0) and the other containing a central cut-out with a cut-out to edge length ratio (c/a) of 0.4. In Table 5, results are obtained first without any elastic foundation ($K_0 = 0$, $K_S = 0$) and later with a plate resting on an elastic foundation having Winkler stiffness parameter (K_0) of 1000 and Pasternak stiffness (K_S) of 100. In the presence of a cut-out, the frequencies of both types of plates, without an elastic foundation and resting on an elastic foundation, tend to increase compared to plates without any cut-out. However, the increase in frequency is significantly more pronounced for plates resting on an elastic foundation than for plates without an elastic foundation.

4.3 Clamped Square isotropic plate resting on elastic foundation with varying stiffness parameter

A square plate with a thickness-to-side ratio of 0.10 and two types of plate cut-out is considered, one without any cut-out and another with a square central

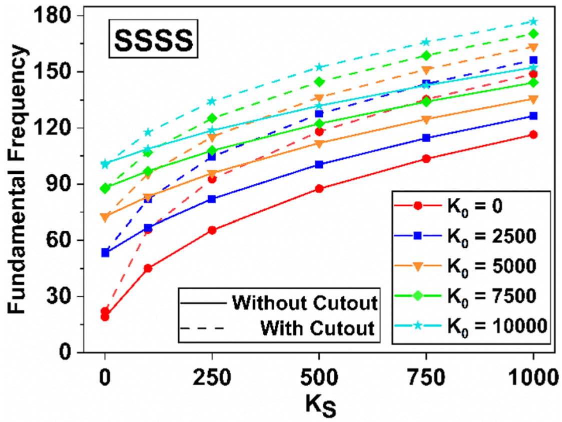

Fig. 6 Comparison of the fundamental frequency of two types of simply supported square isotropic plate, one without cut-out and one with cut-out (c/a = 0.5), with the variation of Pasternak stiffness K_S and Winkler stiffness K_0

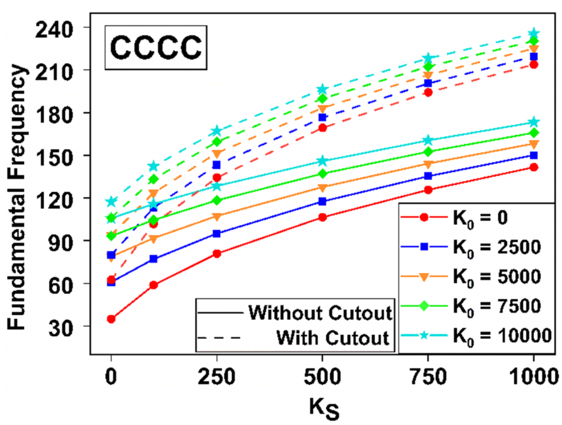

Fig. 7 Comparison of the fundamental frequency of two types of clamped square isotropic plate, one without cut-out and one with cut-out (c/a = 0.5), with the variation of Pasternak stiffness K_S and Winkler stiffness K_0

cut-out of c/a = 0.5. Different elastic foundation models are obtained by varying the elastic foundation stiffness parameter.

The frequencies of the plates plotted in Figs. 6 and 7 are determined for two boundary conditions: a simply supported plate and a clamped square plate. The abscissa represents the variation in the Pasternak stiffness coefficient, while the ordinate represents the non-dimensional frequency. We considered six different Winkler stiffness values for each Pasternak stiffness coefficient in our analysis.

In Figs. 6 and 7, the continuous lines denote the natural frequency of a square plate without any internal cut-out, and the dashed lines give the frequency of a square plate with a central square cut-out. It can be observed that the frequency increases as both the Winkler stiffness and Pasternak stiffness increase. The plate frequency increases rapidly with the increase of Pasternak stiffness compared to an increase in Winkler Stiffness; this shows that the effect of Pasternak stiffness in the elastic foundation model is much more profound than the Winkler stiffness.

4.4 Effect of varying cut-out sizes of a square plate with various boundary conditions

A square isotropic plate containing a square central cut-out, as given in Fig. 2 of various sizes is analyzed for six different boundary conditions, first without elastic foundation (denoted by $K_0 = 0$, $K_S = 0$), and then with two different parameters of elastic foundation ($K_0 = 250$, $K_S = 10$ & $K_0 = 1000$, $K_S = 100$). The obtained non-dimensional fundamental frequencies are plotted in Fig. 8 for the different boundary conditions, and based on the analysis, it can be observed that increasing the cut-out size in plates with four edges clamped or simply supported leads to a decrease in plate stiffness and mass. However, the decrease in mass outweighs the decrease in stiffness, resulting in an increase in the fundamental frequency as the cut-out size increases.

In the case of plates with free edges, increasing the cut-out size causes a decrease in stiffness, subsequently reducing the fundamental frequency at larger cut-out sizes. Nonetheless, the frequencies become similar for larger cut-out sizes between plates with and without a cut-out for plates containing free edges. This finding suggests that the influence of the elastic foundation diminishes as the cut-out size increases in plates containing free edges.

4.5 Effect of increasing the cut-out size in a rectangular plate resting on an elastic foundation with varying elastic stiffness parameter

A simply supported rectangular plate with an aspect ratio (a/b) of 0.5 and a thickness-to-side ratio (h/a) of 0.15 resting on an elastic foundation is analyzed. Fundamental frequencies for different cut-out sizes

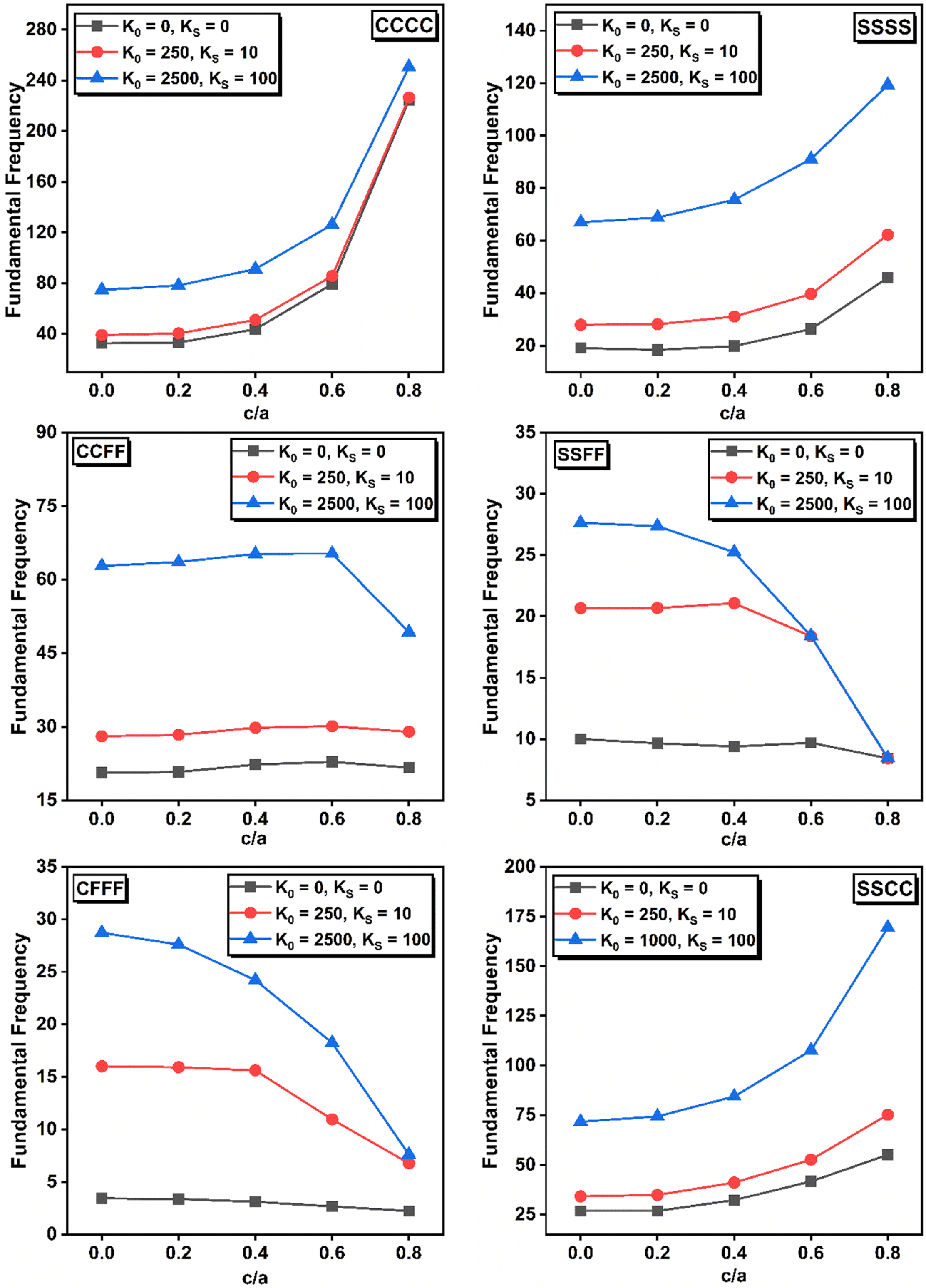

Fig. 8 Effect of the variation of cut-out size and varying elastic foundation parameter on the vibration response of square plate having thickness to side ratio of 0.10 and varying boundary conditions

Table 6 Non-dimensional frequency parameter of a rectangular plate having an aspect ratio (a/b) of 0.5 and thickness-to-side ratio of h/a of 0.15 with varying central cut-out dimensions and various Winkler and Pasternak stiffness parameters

K_0	K_S	c/b	d/b	ω_1	ω_2	ω_3	ω_4	ω_5	ω_6
0	0	0	0	11.7625	18.3372	28.6265	36.3426	41.8772	41.8993
		0.3	0.3	10.7314	17.3632	23.5779	29.1196	38.7978	40.92
			0.5	9.8703	15.7534	17.6084	27.2206	31.489	42.0525
			0.7	9.1117	11.5792	18.3267	24.1911	28.0031	37.7206
			0.9	8.6691	9.1872	18.5147	19.5189	30.1607	31.6332
500	10	0	0	26.9766	31.4966	39.8166	45.9895	51.1368	51.7136
		0.3	0.3	27.3999	30.7668	35.8589	40.6433	48.3836	51.447
			0.5	27.7011	30.8986	31.5919	38.8199	42.3627	52.0397
			0.7	27.7878	28.7623	32.9699	36.826	40.2288	48.0792
			0.9	27.6521	27.7854	33.2286	33.6876	42.316	43.1804
1000	50	0	0	39.8522	46.1735	56.426	59.7551	61.5049	67.4752
		0.3	0.3	41.8434	45.1203	51.4289	57.9381	64.641	69.5304
			0.5	43.3773	46.9217	47.2712	55.4431	58.8716	70.3795
			0.7	44.1454	44.9146	50.4166	53.6635	58.6739	65.8833
			0.9	43.9909	44.0391	50.6699	50.8449	61.1137	61.4679
5000	100	0	0	63.5727	72.4786	76.7802	80.8759	82.1906	89.7171
		0.3	0.3	73.7188	77.6395	78.4269	80.2075	81.2307	84.9031
			0.5	79.6585	80.3081	80.384	81.5688	82.2499	83.1507
			0.7	80.21	80.7141	81.7815	82.1388	83.7844	85.809
			0.9	80.046	80.0677	80.7084	80.7089	85.8377	85.9185

with various elastic stiffness parameters are obtained in Table 6. Introducing a central cut-out in the rectangular plate results in lower fundamental frequencies than a plate without a central cut-out since the stiffness of the plate decreases. However, as the cut-out size increases, the fundamental frequencies increase since the mass decreases.

For plates resting on an elastic foundation, since the stiffness of the plate and the foundation is inherently higher compared to a plate without an elastic foundation, the introduction of a cut-out in the plate decreases the mass without much variation in the stiffness of the plate and results in higher natural frequency with cut-outs.

Further, a square plate resting on an elastic foundation with stiffness parameters of $K_0 = 1000$ and $K_S = 100$ having thickness-to-side ratios of 0.05, 0.10, and 0.20 is considered. Fundamental frequencies are obtained in Tables 7 and 8 for four types of plates, a plate without any cut-out (Plate Type I), a plate with a central cut-out having c/a of 0.4 (Plate Type II) and plates with two different cut-out layouts having four cut-outs of c/a of 0.1 each as given in Fig. 9, i.e., one having cut-outs at four corners (Plate Type III) and other plate having four cut-outs at the mid-length of the edges (Plate Type IV), such that the area of the four cut-outs in the plate remains equal to the area of the central cut-out. The first six natural frequencies are obtained for a square plate and a rectangular plate with an aspect ratio of 2. In the problem, two types of edge conditions are considered, one with all edges simply supported and the other with all edges clamped.

From Tables 7 and 8, where the non-dimensional frequencies are given for a simply supported plate, and a plate with all edges clamped, respectively, we can observe that a plate with centrally located cut-out results in higher frequency than a plate with four cut-outs of the same area as the central cut-out distributed throughout the plate. The higher vibration frequency of a plate with a central cut-out may be attributed to the introduction of smaller cut-outs throughout the plate, resulting in diminished stiffness compared to a plate with a larger centrally located cut-out. The contour plots of the first five vibration modes for all square plates considered with the mentioned cut-outs are given in Fig. 10.

Table 7 Non-dimensional frequency of a simply supported isotropic plate resting on an elastic foundation ($K_0 = 1000$, $K_S = 50$) having aspect ratio a/b = 1, 2 varying the thickness ratio (h/b) and considering three different cut-out conditions with cut-outs having equal mass

a/b	h/b	Plate Type	ω_1	ω_2	ω_3	ω_4	ω_5	ω_6
1	0.05	I	47.396	73.029	75.162	101.273	117.799	121.049
		II	54.979	65.860	68.325	94.696	99.037	133.897
		III	45.101	69.818	72.423	99.399	113.204	121.439
		IV	45.113	69.902	71.696	89.347	112.864	134.361
	0.10	I	46.893	70.555	72.852	95.677	109.347	112.926
		II	53.955	63.364	66.056	89.907	91.391	121.710
		III	44.456	67.123	69.974	93.391	104.524	108.182
		IV	44.494	67.369	68.880	83.512	103.547	103.723
	0.20	I	45.319	61.579	61.578	64.365	67.272	73.356
		II	50.748	57.518	60.929	75.864	78.077	78.077
		III	42.841	54.091	54.093	60.975	63.931	64.659
		IV	42.979	49.637	49.637	59.371	61.623	62.905
2	0.05	I	18.962	25.762	37.459	47.633	53.941	54.534
		II	21.806	25.199	33.030	39.811	48.735	58.513
		III	17.490	23.000	34.466	45.142	50.086	50.099
		IV	17.258	24.762	37.194	40.908	44.827	52.522
	0.10	I	18.790	25.318	36.307	45.736	51.326	51.944
		II	21.535	24.633	31.651	37.973	46.440	55.369
		III	17.183	22.299	33.054	43.117	47.253	47.331
		IV	16.938	24.231	35.833	38.648	41.745	49.673
	0.20	I	18.213	23.919	33.018	40.710	41.474	44.659
		II	20.645	23.095	28.652	33.645	40.937	47.715
		III	16.465	20.702	29.724	36.910	38.273	40.996
		IV	16.197	22.901	32.422	33.662	33.844	35.710

4.6 Effect of symmetricity of cut-out position

The effect of the symmetricity of the cut-out layouts in the square simply supported plate is considered in this section. Five types of cut-out layouts are considered, as given in Fig. 11, with each having the same cut-out area-to-plate area ratio. The non-dimensional fundamental frequency for each cut-out type is obtained for a plate without an elastic foundation and with an elastic foundation having stiffness parameters of $K_0 = 1000$ and $K_S = 100$. The non-dimensional fundamental frequencies are plotted in Fig. 12, where it can be observed that symmetric concentrated cut-outs (Type I) exhibit higher fundamental frequencies compared to plates with asymmetric concentrated cut-out layouts (Type II and III), regardless of the presence of elastic foundation. However, when the cut-out is distributed around the plate area (Type IV and V), the fundamental frequencies tend to be lower than when the cut-out is concentrated in a single area, even though the area of the cut-outs remains the same in all cases. Furthermore, the asymmetrically distributed cut-out layout (Type V) registers a slightly higher fundamental frequency when the plate has no elastic foundation. In comparison, the symmetrically distributed cut-out layout (Type IV) exhibits a slightly higher fundamental frequency when the plate rests on an elastic foundation.

Table 8 Non-dimensional frequency of a clamped isotropic plate resting on an elastic foundation ($K_0 = 1000$, $K_S = 50$) having aspect ratio a/b = 1, 2 varying the thickness ratio (h/b) and considering three different cut-out conditions with cut-outs having equal mass

a/b	h/b	Plate type	ω_1	ω_2	ω_3	ω_4	ω_5	ω_6
1	0.05	I	57.923	92.346	92.684	124.014	144.406	145.324
		II	75.600	86.937	87.349	116.863	117.164	157.171
		III	55.833	88.574	88.903	117.419	141.497	142.422
		IV	52.369	85.741	85.880	112.430	140.380	150.596
	0.10	I	55.776	85.128	85.796	111.099	123.155	123.160
		II	70.923	79.943	80.733	103.724	105.307	135.908
		III	53.753	81.708	82.360	105.614	108.183	108.186
		IV	50.422	79.636	79.880	99.273	99.273	100.971
	0.20	I	51.057	61.578	61.578	71.461	73.352	73.384
		II	61.588	67.295	69.499	75.864	78.076	78.077
		III	49.117	54.091	54.092	64.856	68.548	70.530
		IV	46.754	49.637	49.637	59.372	68.455	69.030
2	0.05	I	28.735	36.130	48.757	66.376	66.376	73.052
		II	36.423	37.194	53.857	57.595	67.098	76.153
		III	27.037	32.155	44.114	60.732	61.748	62.694
		IV	23.791	34.916	47.904	53.379	61.302	66.173
	0.10	I	27.523	34.304	45.640	60.319	60.969	65.964
		II	34.466	35.013	49.704	52.798	60.892	68.673
		III	25.820	30.383	41.199	55.023	56.548	56.779
		IV	22.566	33.145	44.773	48.611	55.123	59.136
	0.20	I	24.350	29.810	38.465	41.475	47.870	49.482
		II	29.785	30.101	41.137	43.318	48.776	53.982
		III	22.729	26.265	34.813	36.909	43.287	43.862
		IV	19.968	29.046	33.662	38.189	38.363	39.690

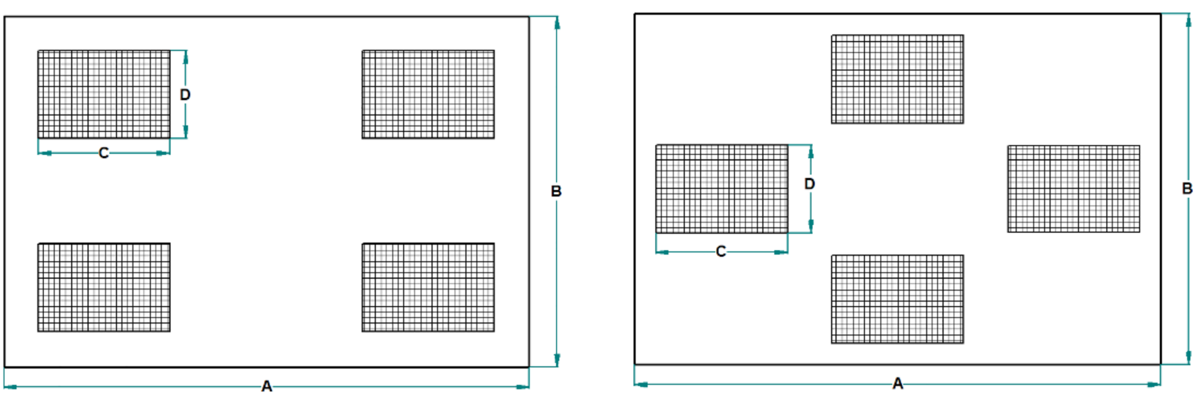

Fig. 9 Plate containing four equal-sized square cut-outs (c/a = 0.1) at two different layouts

4.7 Effect of thickness-to-side ratio and changing cut-out size on the vibration response of a square plate

A square isotropic plate with different boundary conditions is analyzed, varying the thickness-to-side (h/a) ratio and the cut-out-to-edge length (c/a) ratio. Three conditions of elastic foundations are analyzed. In one case, the elastic foundation is not considered; in the other two, the elastic foundation with stiffness parameters ($K_0 = 1000$, $K_S = 25$) and ($K_0 = 4000$, $K_S = 100$) is considered. The fundamental frequencies are plotted

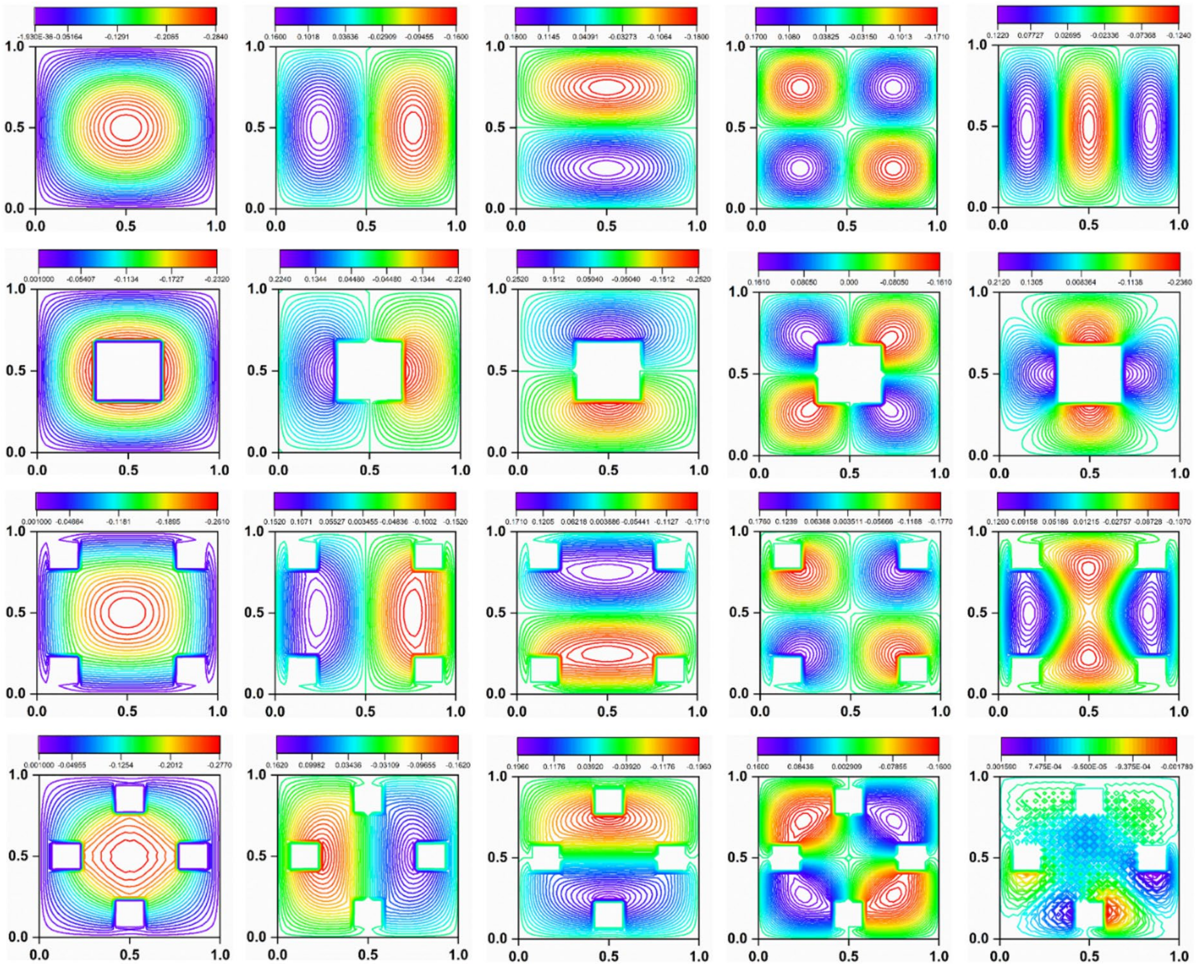

Fig. 10 First five contour plots of the free vibration of a square plate resting on an elastic foundation having stiffness parameters $K_0 = 1000$ and $K_S = 100$ and thickness to side ratio (h/a) of 0.10, for four types of plate, plate without cut-out, a plate having central square cut-out of c/a = 0.4 and plate with four equal-sized square cut-outs of c/a = 0.1 at two different layouts

for various boundary conditions and cut-out dimensions in Fig. 13, and it can be observed that when the plate is clamped on four edges, the frequency increases as the cut-out size increases for all plate thickness ratios. The findings suggest that even as the cut-out size increases and the mass decreases, the stiffness of the plate remains significant, leading to an increase in the vibration frequency. For plates resting on an elastic foundation, specifically those with four edges simply supported or two edges simply supported and two edges clamped, the vibration frequency initially increases with larger cut-out sizes, considering various thickness-to-side ratios. This initial increase in frequency is due to the decrease in plate mass. However, as the cut-out size further increases, the stiffness of the plate decreases significantly, resulting in a decrease in

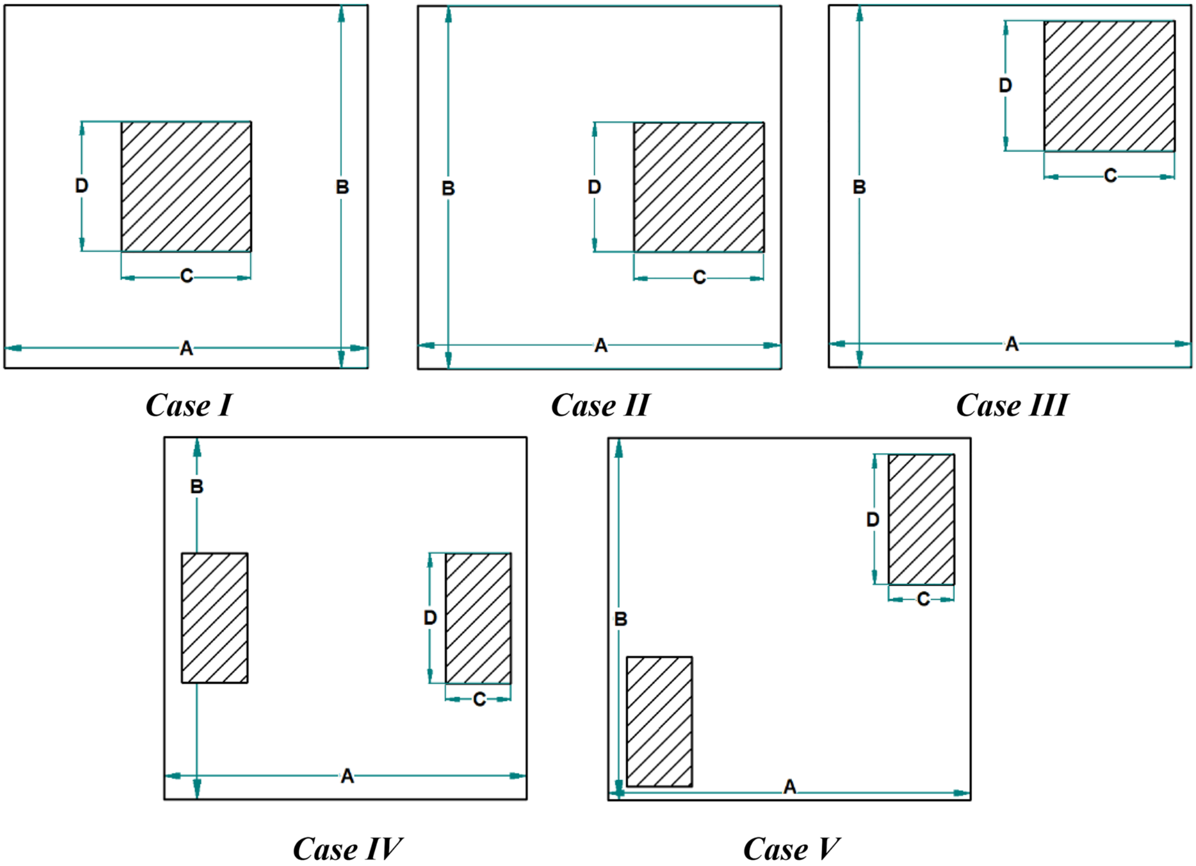

Fig. 11 Different types of symmetric (Case I and IV) and asymmetric (Case II, III, V) cut-outs in a square plate having the same cut-out to plate area (c/a) ratio of 0.4

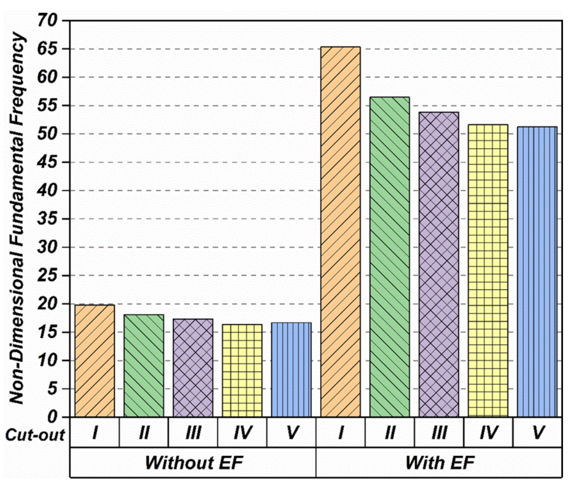

Fig. 12 Fundamental frequency of a simply supported square isotropic plate without elastic foundation (EF) and with elastic foundation with different types of cut-out arrangements with the same cut-out to the plate area ratio

frequency for moderately thick and thick plates. In the case of thin plates with an elastic foundation, increasing the cut-out size leads to a decrease in plate mass while maintaining significant plate stiffness. As a result, the obtained frequency increases. On the other hand, for cantilever plates, as the cut-out size increases, the decrease in plate stiffness is more prominent compared to the decrease in plate mass. Consequently, the fundamental frequency decreases.

4.8 Applicability of present finite element formulation to rectangular plates containing cut-outs of irregular shapes

The present formulation is used to compare the results obtained by Ovesy and Fazilati (2012), who used the Finite Strip Method (FSM) to obtain results for a square isotropic plate with circular cut-outs of diameter (d) to edge length (a) ratio of

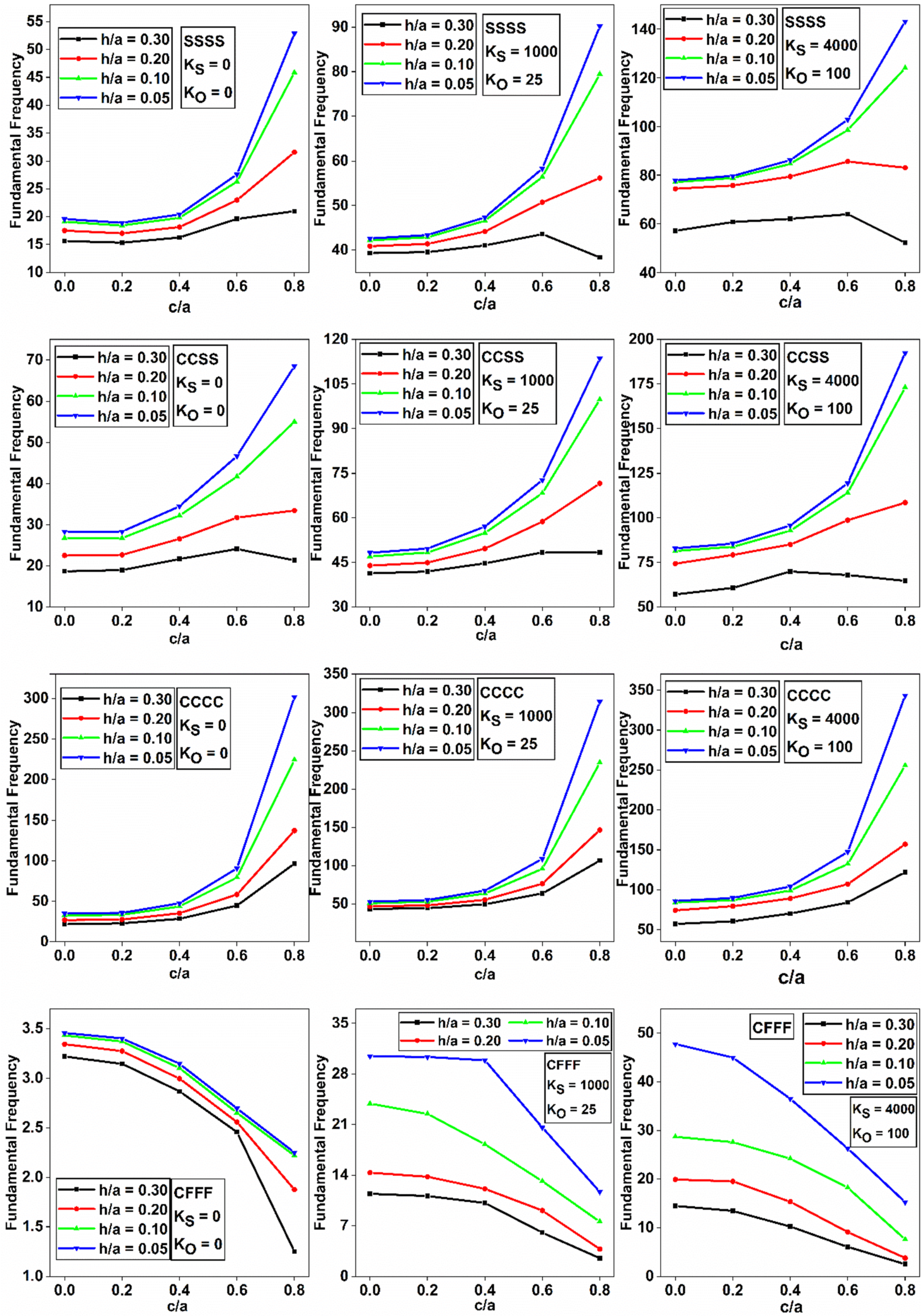

Fig. 13 Variation of the fundamental frequency of a square isotropic plate with varying boundary conditions, central cut-out dimensions, h/a ratios, and elastic foundation stiffness parameters

Table 9 First two frequencies (rad/s) of free vibration of a simply supported isotropic plate containing circular cut-out of d/a = 0.5 without elastic foundation and with an elastic foundation of stiffness parameter $K_0 = 1000$ and $K_S = 10$

Mode	Ovesy and Fazilati			Present	Present
	HSDT S-a FSM	Simplified FEM Model	Real FEM model	$\omega\left(\frac{rad}{s}\right)$	With Elastic Foundation ($K_0 = 1000$ and $K_S = 10$) $\omega\left(\frac{rad}{s}\right)$
1	345.524	337.055	337.055	338.465	664.962
2	687.236	636.097	652.381	636.030	858.703

Plate thickness to edge length ratio (h/a) = 0.01, E = 70 GPa, $\rho = 2700$ kg/m^3 and $\upsilon = 0.3$

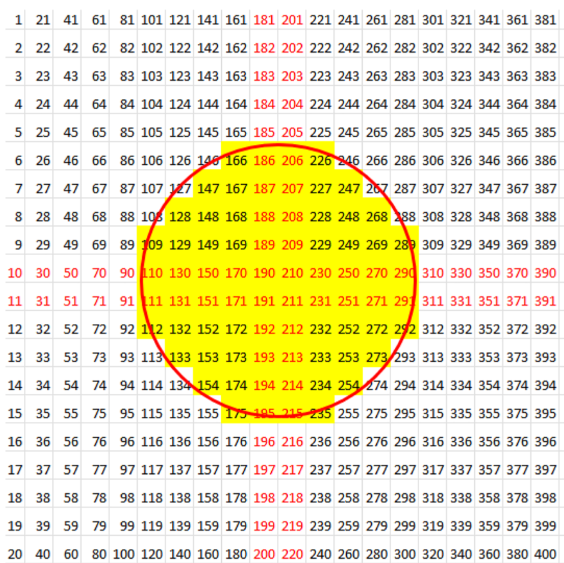

1	21	41	61	81	101	121	141	161	181	201	221	241	261	281	301	321	341	361	381
2	22	42	62	82	102	122	142	162	182	202	222	242	262	282	302	322	342	362	382
3	23	43	63	83	103	123	143	163	183	203	223	243	263	283	303	323	343	363	383
4	24	44	64	84	104	124	144	164	184	204	224	244	264	284	304	324	344	364	384
5	25	45	65	85	105	125	145	165	185	205	225	245	265	285	305	325	345	365	385
6	26	46	66	86	106	126	146	166	186	206	226	246	266	286	306	326	346	366	386
7	27	47	67	87	107	127	147	167	187	207	227	247	267	287	307	327	347	367	387
8	28	48	68	88	108	128	148	168	188	208	228	248	268	288	308	328	348	368	388
9	29	49	69	89	109	129	149	169	189	209	229	249	269	289	309	329	349	369	389
10	30	50	70	90	110	130	150	170	190	210	230	250	270	290	310	330	350	370	390
11	31	51	71	91	111	131	151	171	191	211	231	251	271	291	311	331	351	371	391
12	32	52	72	92	112	132	152	172	192	212	232	252	272	292	312	332	352	372	392
13	33	53	73	93	113	133	153	173	193	213	233	253	273	293	313	333	353	373	393
14	34	54	74	94	114	134	154	174	194	214	234	254	274	294	314	334	354	374	394
15	35	55	75	95	115	135	155	175	195	215	235	255	275	295	315	335	355	375	395
16	36	56	76	96	116	136	156	176	196	216	236	256	276	296	316	336	356	376	396
17	37	57	77	97	117	137	157	177	197	217	237	257	277	297	317	337	357	377	397
18	38	58	78	98	118	138	158	178	198	218	238	258	278	298	318	338	358	378	398
19	39	59	79	99	119	139	159	179	199	219	239	259	279	299	319	339	359	379	399
20	40	60	80	100	120	140	160	180	200	220	240	260	280	300	320	340	360	380	400

Fig. 14 Elements in a square plate containing circular cut-out, highlighted elements inside the circular ring are neglected while obtaining the total energy of the plate

0.5. The results obtained are given in Table 9, and the cut-out elements in the present model using a 20 × 20 mesh are selected such that the cut-out elements roughly mimic the circular cut-out area of the real FEM model as shown in Fig. 14. The fundamental frequency obtained using the present formulation stands in good agreement with the results obtained by Ovesy and Fazilati, who considered a simply supported plate on all the edges without elastic foundation. Also, the results are obtained for a similar plate with a circular cut-out and resting on an elastic foundation having stiffness parameters $K_0 = 1000$ and $K_S = 10$. Therefore, it can be concluded that the present formulation can be used for cut-outs of irregular shapes, and the accuracy of the present method for irregular shapes increases as the mesh size increases.

5 Conclusion

Extensive work has been done on the vibration analysis of different types of plates, having different geometrical dimensions and material properties, with different boundary conditions, and on plates resting on elastic foundations. However, the dynamic behavior of cut-out plates or plates containing cut-outs differs from that of a solid plate without any cut-outs, as observed in earlier studies in the literature review. The dynamic behavior of cut-out plates resting on an elastic foundation and the interaction between cut-out elements and the elastic foundation has not been analyzed earlier. Therefore, this work attempts to analyze the vibration response of cut-out elements resting on an elastic foundation using the Finite Element Method (FEM) and the First Order Shear Deformation theory, and there lies the novelty of the present work. The primary outcomes of the present work are listed below.

1. The inclusion of rotary inertia in the finite element formulation accurately predicts the fundamental frequency for both thin and thick plates. Mass matrix with rotary inertia is applicable for both thick and thin plates, and mass matrix without rotary inertia is valid only for thin plates.
2. The effect of the elastic foundation in the free vibration of plates is increased natural frequencies and decreased transverse deflection of the plates.

3. As the Winkler and Pasternak stiffness coefficient increases, the plate frequency increases because the stiffness of the plate increases. A slight increase of Pasternak stiffness results in more increment of fundamental frequency compared to a similar increase of Winkler stiffness coefficient.
4. Cut-outs decrease the mass and stiffness of the plate with simply supported and clamped edges; however, at a small cut-out size for a thick plate, the mass decreases more significantly than the plate's stiffness, which results in higher frequencies of vibration, at larger cut-out size the stiffness decreases and the frequency reduces.
5. For plates with free edges, an increase in cut-out size diminishes the plate stiffness and mass, resulting in lower frequencies than a plate without a cut-out.
6. Distribution of cut-outs throughout the plate results in lower stiffness for both simply supported and clamped plates compared to a plate with the same area of a central cut-out.
7. As the cut-out size increases in thick plates, the vibration frequency decreases since the plate stiffness decreases. However, increasing the cut-out size does not cause a significant decrease in the stiffness of thin and moderately thick plates.
8. For plates with concentrated cut-outs, both with and without elastic foundation, symmetricity of the cut-out position in the plate significantly influences the vibration response of the plate. However, no such definitive conclusion could be made for plates containing distributed cut-outs.
9. The present formulation is best suited for plates containing rectangular cut-outs resting on an elastic foundation; however, the formulation can be extended to study the rectangular plates containing cut-outs of arbitrary shapes to an adequate level of accuracy, which can be further improved using finer meshing at the cost of increased computation times.

The current finite element formulation for rectangular and square plates is described in this article. Future studies, however, can concentrate on adapting the formulation to increase its applicability to examine plates with unusual forms, like skew plates and rhomboid plates. The formulation could also be improved by including time-dependent force and displacement functions in the equations of motion, as well as external excitation effects. This would allow for the thorough investigation of harmonic and transient transverse forced vibrations in plates with cut-outs and elastic foundations.

Declarations

Conflict of interest The authors, in accordance with their ethical obligation as researchers, confirms that there are no relevant financial or non-financial competing interests to report.

References

Akhavan, H., Hashemi, S.H., Taher, H.R.D., Alibeigloo, A., Vahabi, S.: Exact solutions for rectangular Mindlin plates under in-plane loads resting on Pasternak elastic foundation. Part II: frequency analysis. Comput. Mater. Sci. **44**(3), 951–961 (2009). https://doi.org/10.1016/j.commatsci.2008.07.001

Aksu, G.: Free vibration analysis of rectangular plates with cut-outs allowing for transverse shear deformation and rotary inertia. Earthq. Eng. Struct. Dyn. **12**(5), 709–714 (1984). https://doi.org/10.1002/eqe.4290120510

Ali, R., Atwal, S.J.: Prediction of natural frequencies of vibration of rectangular plates with rectangular cutouts. Comput. Struct. **12**(6), 819–823 (1980). https://doi.org/10.1016/0045-7949(80)90019-X

Alipour, M.M., Shariyat, M., Shaban, M.: A semi-analytical solution for free vibration of variable thickness two-directional-functionally graded plates on elastic foundations. Int. J. Mech. Mater. Des. **6**(4), 293–304 (2010). https://doi.org/10.1007/s10999-010-9134-2

Alsebai, F., Al Mukahal, F.H.H., Sobhy, M.: Semi-analytical solution for thermo-piezoelectric bending of FG porous plates reinforced with graphene platelets. Mathematics **10**(21), 1–30 (2022). https://doi.org/10.3390/math10214104

Atmane, H.A., Tounsi, A., Mechab, I., Bedia, E.A.A.: Free vibration analysis of functionally graded plates resting on Winkler-Pasternak elastic foundations using a new shear deformation theory. Int. J. Mech. Mater. Des. **6**(2), 113–121 (2010). https://doi.org/10.1007/s10999-010-9110-x

Datta, P., Ray, M.C.: Finite element analysis of laminated composite plates using zeroth-order shear deformation theory. Int. J. Mech. Mater. Des. **12**(3), 387–400 (2016). https://doi.org/10.1007/s10999-015-9307-0

Dehghan, M., Baradaran, G.H.: Buckling and free vibration analysis of thick rectangular plates resting on elastic foundation using mixed finite element and differential quadrature method. Appl. Math. Comput. **218**(6), 2772–2784 (2011). https://doi.org/10.1016/j.amc.2011.08.020

Guo, H., Zheng, H.: The linear analysis of thin shell problems using the numerical manifold method. Thin Walled Struct. **124**(December), 366–383 (2018). https://doi.org/10.1016/j.tws.2017.12.027

Guo, H., Zheng, H., Zhuang, X.: Numerical manifold method for vibration analysis of Kirchhoff's plates of arbitrary geometry. Appl. Math. Model. **66**, 695–727 (2019a). https://doi.org/10.1016/j.apm.2018.10.006
Guo, H., Zhuang, X., Rabczuk, T.: A deep collocation method for the bending analysis of Kirchhoff plate. Comput. Mater. Contin. **59**(2), 433–456 (2019b). https://doi.org/10.32604/cmc.2019.06660
Guo, H., Lin, S., Zheng, H.: GMLS-based numerical manifold method in mechanical analysis of thin plates with complicated shape or cutouts. Eng. Anal. Bound. Elem. **151**(January), 597–623 (2023). https://doi.org/10.1016/j.enganabound.2023.03.028
Haldar, S.: Free vibration of composite skewed cylindrical shell panel by finite element method. J. Sound Vib. **311**(1–2), 9–19 (2008). https://doi.org/10.1016/j.jsv.2007.08.022
Haldar, S., Sheikh, A.H.: Free vibration analysis of isotropic and composite folded plates using a shear flexible element. Finite Elem. Anal. Des. **42**(3), 208–226 (2005). https://doi.org/10.1016/j.finel.2005.06.003
Huang, M.H., Thambiratnam, D.P.: Analysis of plate resting on elastic supports and elastic foundation by finite strip method. Comput. Struct. **79**(29–30), 2547–2557 (2001). https://doi.org/10.1016/S0045-7949(01)00134-1
Iosilevich, A., Bathe, K.-J., Brezzi, F.: On evaluating the inf-sup condition for plate bending elements. Int. J. Numer. Methods Eng. **40**(19), 3639–3663 (1997). https://doi.org/10.1002/(SICI)1097-0207(19971015)40:19%3c3639::AID-NME232%3e3.0.CO;2-H
Jahromi, H.N., Aghdam, M.M., Fallah, A.: Free vibration analysis of Mindlin plates partially resting on Pasternak foundation. Int. J. Mech. Sci. **75**, 1–7 (2013). https://doi.org/10.1016/j.ijmecsci.2013.06.001
Joodaky, A., Joodaky, I.: A semi-analytical study on static behavior of thin skew plates on Winkler and Pasternak foundations. Int. J. Mech. Sci. **100**, 322–327 (2015). https://doi.org/10.1016/j.ijmecsci.2015.06.025
Kalita, K., Haldar, S.: Parametric study on thick plate vibration using FSDT (2015).
Kalita, K., Haldar, S.: Natural frequencies of rectangular plate with- and without-rotary inertia. J. Inst. Eng. Ser. C **99**(5), 539–555 (2018). https://doi.org/10.1007/s40032-016-0327-9
Lee, L.T., Lee, D.C.: Free vibration of rectangular plates on elastic point supports with the application of a new type of admissible function. Comput. Struct. **65**(2), 149–156 (1997). https://doi.org/10.1016/S0045-7949(96)00426-9
Lee, H.P., Lim, S.P., Chow, S.T.: Effect of transverse shear deformation and rotary inertia on the natural frequencies of rectangular plates with cutouts. Int. J. Solids Struct. **29**(11), 1351–1359 (1992). https://doi.org/10.1016/0020-7683(92)90083-6
Li, J., Huo, Q., Li, X., Kong, X., Wu, W.: Vibration analyses of laminated composite beams using refined higher-order shear deformation theory. Int. J. Mech. Mater. Des. **10**(1), 43–52 (2014). https://doi.org/10.1007/s10999-013-9229-7
Matsunaga, H.: Vibration and stability of thick plates on elastic foundations. J. Eng. Mech. **126**(1), 27–34 (2000). https://doi.org/10.1061/(ASCE)0733-9399(2000)126:1(27)
Nagino, H., Mikami, T., Mizusawa, T.: Three-dimensional free vibration analysis of isotropic rectangular plates using the B-spline Ritz method. J. Sound Vib. **317**(1–2), 329–353 (2008). https://doi.org/10.1016/j.jsv.2008.03.021
Ovesy, H.R., Fazilati, J.: Buckling and free vibration finite strip analysis of composite plates with cutout based on two different modeling approaches. Compos. Struct. **94**(3), 1250–1258 (2012). https://doi.org/10.1016/j.compstruct.2011.11.009
Pal, S., Haldar, S., Kalita, K.: Dynamic analysis of plates with cut-out carrying concentrated and distributed mass. Int. J. Marit. Eng. **162**(A3), 263–276 (2021a). https://doi.org/10.5750/ijme.v162ia3.1136
Pal, S., Bose, C., Haldar, S.: Free vibration analysis of laminated composite plate with cut-out carrying concentrated and distributed mass. J. Inst. Eng. Ser. C **102**(6), 1447–1460 (2021b). https://doi.org/10.1007/s40032-021-00747-y
Qin, X., Jin, G., Chen, M., Yin, S.: Free in-plane vibration analysis of circular, annular, and sector plates using isogeometric approach. Shock Vib. **100**, 200 (2018). https://doi.org/10.1155/2018/4314761
Rajamani, A., Prabhakaran, R.: Dynamic response of composite plates with cut-outs, part I: simply-supported plates. J. Sound Vib. **54**(4), 549–564 (1977). https://doi.org/10.1016/0022-460X(77)90612-5
Ray, M.C.: Three-dimensional exact elasticity solutions for antisymmetric angle-ply laminated composite plates. Int. J. Mech. Mater. Des. **17**(4), 767–782 (2021). https://doi.org/10.1007/s10999-021-09536-y
Reddy, J.N.: Large amplitude flexural vibration of layered composite plates with cutouts. J. Sound Vib. **83**(1), 1–10 (1982). https://doi.org/10.1016/S0022-460X(82)80071-0
Reddy, J.N.: A Simple Higher-Order Theory for Laminated Composite Plates. J. Appl. Mech. **51**(4), 745–752 (1984). https://doi.org/10.1115/1.3167719
Sayyad, A.S., Ghugal, Y.M.: A new shear and normal deformation theory for isotropic, transversely isotropic, laminated composite and sandwich plates. Int. J. Mech. Mater. Des. **10**(3), 247–267 (2014). https://doi.org/10.1007/s10999-014-9244-3
Sivakumar, K., Iyengar, N.G.R., Deb, K.: Free vibration of laminated composite plates with cutout. J. Sound Vib. **221**(3), 443–470 (1999). https://doi.org/10.1006/jsvi.1998.2034
Sun, X., Zhang, P., Qiao, H., Lin, K.: High-order free vibration analysis of elastic plates with multiple cutouts. Arch. Appl. Mech. **91**(4), 1837–1858 (2021). https://doi.org/10.1007/s00419-020-01857-2
Thai, H.T., Park, M., Choi, D.H.: A simple refined theory for bending, buckling, and vibration of thick plates resting on elastic foundation. Int. J. Mech. Sci. **73**, 40–52 (2013). https://doi.org/10.1016/j.ijmecsci.2013.03.017
Van Vu, T., Curiel-Sosa, J.L., Bui, T.Q.: A refined sin hyperbolic shear deformation theory for sandwich FG plates by enhanced meshfree with new correlation function. Int. J. Mech. Mater. Des. **15**(3), 647–669 (2019). https://doi.org/10.1007/s10999-018-9430-9
Xiang, Y.: Vibration of rectangular Mindlin plates resting on non-homogenous elastic foundations. Int. J. Mech. Sci. **45**(6–7), 1229–1244 (2003). https://doi.org/10.1016/S0020-7403(03)00141-3

Xue, Y., Jin, G., Ding, H., Chen, M.: Free vibration analysis of in-plane functionally graded plates using a refined plate theory and isogeometric approach. Compos. Struct. **192**(December), 193–205 (2018). https://doi.org/10.1016/j.compstruct.2018.02.076

Ye, T., Jin, G., Su, Z., Chen, Y.: A modified Fourier solution for vibration analysis of moderately thick laminated plates with general boundary restraints and internal line supports. Int. J. Mech. Sci. **80**, 29–46 (2014). https://doi.org/10.1016/j.ijmecsci.2014.01.001

Zarouni, E., Jalilian Rad, M., Tohidi, H.: Free vibration analysis of fiber reinforced composite conical shells resting on Pasternak-type elastic foundation using Ritz and Galerkin methods. Int. J. Mech. Mater. Des. **10**(4), 421–438 (2014). https://doi.org/10.1007/s10999-014-9254-1

Zenkour, A.M., Allam, M.N.M., Shaker, M.O., Radwan, A.F.: On the simple and mixed first-order theories for plates resting on elastic foundations. Acta Mech. **220**(1–4), 33–46 (2011). https://doi.org/10.1007/s00707-011-0453-7

Zenkour, A.M., Allam, M.N.M., Radwan, A.F.: Bending of cross-ply laminated plates resting on elastic foundations under thermo-mechanical loading. Int. J. Mech. Mater. Des. **9**(3), 239–251 (2013). https://doi.org/10.1007/s10999-012-9212-8

Zhou, D., Cheung, Y.K., Lo, S.H., Au, F.T.K.: Three-dimensional vibration analysis of rectangular thick plates on Pasternak foundation. Int. J. Numer. Methods Eng. **59**(10), 1313–1334 (2004). https://doi.org/10.1002/nme.915

Zhuang, X., Guo, H., Alajlan, N., Zhu, H., Rabczuk, T.: Deep autoencoder based energy method for the bending, vibration, and buckling analysis of Kirchhoff plates with transfer learning. Eur. J. Mech. A Solids **87**(January), 104225 (2021). https://doi.org/10.1016/j.euromechsol.2021.104225